Available online at www.sciencedirect.com
ScienceDirect
International Journal of Mass Spectrometry 272 (2008) 99–118
International Journal of Mass Spectrometry
www.elsevier.com/locate/ijms

Review

Structures, energetics and spectroscopy of gas phase transition metal ion–benzene complexes

Michael A. Duncan *

Department of Chemistry, University of Georgia, Athens, GA 30602-2556, USA

Received 3 December 2007; received in revised form 16 January 2008; accepted 17 January 2008
Available online 10 March 2008

Abstract

Metal–benzene complexes provide classic examples of organometallic chemistry, and their ions have similar appeal for mass spectrometry and ion chemistry. This review covers new formation methods for the generation of novel metal ion–benzene complexes and clusters in the gas phase, as well as new measurements of their properties. Collision induced dissociation, radiative decay kinetics and photodissociation methods have been applied to determine bonding energetics, while UV–vis, infrared and photoelectron spectroscopic measurements have been applied to determine structure and bonding patterns. Electronic structure calculations have been pursued to complement these various experiments. This review surveys recent progress in these areas, providing an overview of the field and suggesting future research directions.

Keywords: Organometallic ion; Photodissociation; Infrared spectroscopy; Cluster

Contents

1. Introduction

The special bonding between transition metal cations and benzene was recognized early on in the history of organometallic chemistry. The addition of metal salts to liquid benzene produced colored solutions, which were soon interpreted to arise from metal–benzene complexes [1–6]. When species such as ferrocene [7,8] and di-benzene chromium [9] were synthesized directly and found to be especially stable, the concept of the 18-electron rule and its role in electronic structure was recognized, and variations on this theme were explored. A number of spectroscopic methods from conventional chemistry were applied to these systems over the years, and systematic concepts about stability were developed [10–19]. Although sandwich structures having the metal on or near the sixfold symmetry axis were most common, it was also found in the early work that late transition metals such as ruthenium might adopt lower symmetry and/or lower coordinated (η_2 or η_4) structures [20]. In recent years, many of the same concepts explored in conventional organometallic chemistry have been extended to the gas phase environment of mass spectrometry [21–24]. This is especially true for metal–benzene complexes, whose ions have been

* Tel.: +1 706 542 1998.
E-mail address: maduncan@uga.edu.

1387-3806/$ – see front matter © 2008 Elsevier B.V. All rights reserved.
doi:10.1016/j.ijms.2008.01.010

studied extensively. This review article focuses on metal ion benzene complexes and the many recent experiments that have investigated the structure and bonding in these prototypical organometallic complexes. Although these systems are somewhat well-studied, they still provide challenges to theory and they are convenient models for more complex metal π bonding, as found in intercalated metal materials and in the bonding of metals at aromatic surfaces (e.g., polycyclic aromatics, carbon nanotubes).

Transition metal ions can be produced in the gas phase via volatile precursors (e.g., carbonyls), metal oven sources, ion sputtering, etc. Using these methods, metal ion–benzene complexes have been produced for many years in mass spectrometry experiments [21–24]. Early work focused on the formation reactions that generated these complexes, followed by reactions of the metal–benzene ions with other systems. In some cases, metal mediated chemistry made it possible to produce benzene from smaller hydrocarbon precursors, e.g., ethylene [25]. More detailed examinations of the chemistry of these systems has been covered elsewhere [21–25], and are beyond the scope of the present article. A critical juncture for this field occurred with the introduction of the laser vaporization source by Smalley and coworkers [26]. Over the last 20 years or so, the production of metal ions and metal clusters in the gas phase has become extremely efficient using this methodology. Virtually any transition metal that is available in powder, solid rod or disk form can now be produced in high densities in any kind of mass spectrometer. Even weakly bound ions can also be cooled and stabilized via collisions using pulsed nozzle cluster sources. Because of the higher metal densities available, metal-molecular ion–molecule complexes such as those with benzene can be produced and studied under well-defined conditions. Investigations using more sophisticated mass spectrometry methods and ion manipulation have become possible, including experiments designed to measure bonding energetics, spectroscopy and structures. It is these latter areas that are the focus of this review on transition metal ion–benzene complexes. Complementing this new experimental work, there have been many computational studies of the electronic and geometric structures of metal ion–benzene complexes, as well as their bonding energetics and spectroscopy [27–42].

2. Mass spectrometry distributions

Simple adducts between metal ions and benzene have been seen for many years in mass spectrometers [21–24]. In situations in which higher vapor pressures of benzene were present, di-benzene adducts could also be produced. Because of the known stability of species such as di-benzene chromium from condensed phase studies, these adducts were not surprising, and many studies were carried out to investigate their formation rates, equilibrium concentrations, collisional dissociation energies and photodissociation processes. These experiments are discussed below in later sections of this paper. However, significant insight into the stabilities of metal ion benzene complexes began to be found when laser vaporization processes in pulsed nozzle supersonic expansion sources were first combined with mass spectrometry detection [26]. In these experiments, the greater metal concentration and cooling provided by this new environment made it possible to produce larger complexes containing more benzene molecules. It also became possible to produce clusters with multiple metal atoms and multiple benzene molecules.

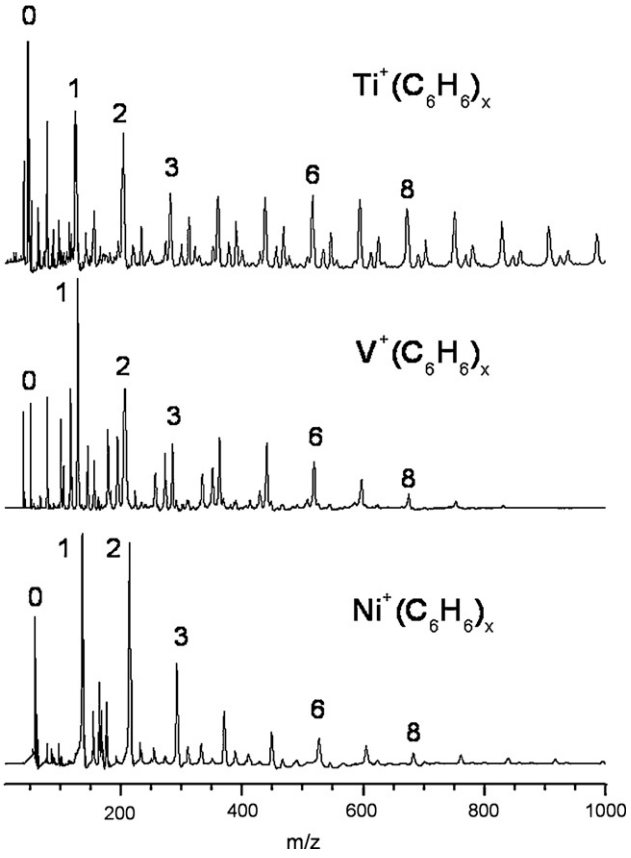

Fig. 1. The mass spectra of metal ion–benzene complexes of titanium, vanadium and nickel.

Fig. 1 shows an example of the kind of mass spectra that can be produced via a laser vaporization source with a pulsed nozzle expansion [43]. In these three mass spectra for titanium, vanadium and nickel systems, complexes that each contain a single metal cation with 6–8 or more benzene molecules are produced. These spectra represent the cation complexes that grew directly form the cluster source; there is no post-ionization process. Cation clusters are entrained in the expansion gas flow, collimated into a molecular beam by a skimmer, and then they flow into a second chamber which houses a mass spectrometer. Cations are sampled with pulsed acceleration plates into the time-of-flight mass spectrometer situated perpendicular to the molecular beam axis. The spectra contain a number of masses other than metal–benzene adducts, including fragmentation products and impurities from the expansion gas. A small amount of water is added as an electron scavenger to enhance the ion yield, and water-containing ions are also present. At the low temperatures of these expansions, electron-ion recombination can be efficient, which tends to neutralize the clusters formed, but experience has shown that a small amount of water can limit the neutralization processes. However, the main progressions of

masses seen here correspond to ion–molecule complexes of the form $M^+(benzene)_n$. These mass spectra were generated using a so-called "cutaway" cluster source developed in our lab, in which the laser vaporization spark is positioned immediately at the exit point of the supersonic expansion of gas. There is no confinement of the metal vapor downstream from this point. This makes a colder expansion, but there are fewer metal–metal collisions, and very little formation of clusters containing multiple metal atoms.

Multiple metal atom clusters were produced previously from electron impact ionization of volatile organometallics, from oven sources or from sputtering sources [21–24,44,45]. However, the laser vaporization source is much more efficient for metal cluster production and it is general for many metal systems [26]. To make such larger metal atom clusters by laser vaporization, a suitable sample (rod, disk, etc.) is mounted on the front of a gas valve, similar to the configuration used above for $M^+(benzene)_n$ complexes, but a so-called "growth channel" is added to the gas flow beyond the laser vaporization point [26]. Metal clusters or metal cluster ions containing up to several hundred atoms can be produced by this method. The extent of the clustering can be controlled with the vaporization laser power and wavelength, the pressure of the expansion gas, the duration of the gas pulse and the specific configuration (length and diameter) of the growth channel. Using sputtering methods or laser vaporization sources, reactions of multiple metal atom clusters with benzene have been studied by several research groups [46–49]. Production of benzene from smaller hydrocarbons has been observed [45], and chemisorption or dehydrogenation reactions were found to vary with the number of metal atoms in the cluster for several different metal systems [46–49].

Perhaps the most spectacular results from the mass spectrometry of metal–benzene complexes is found in the work of Kaya, Nakajima and coworkers [50–55]. In studies in which clusters were produced containing multiple transition metal atoms and multiple benzene molecules, dramatic preferences were observed for species with $[M_n(benzene)_{n+1}]^+$ stoichiometries. This preference was most apparent for the early transition metals such as titanium and vanadium, but it was found for several metal systems. An example mass spectrum showing this behavior is presented in Fig. 2. Because of the striking stoichiometry in these clusters, their structures were proposed to be based on the sandwich motif, in which the first member would be the familiar $M(benzene)_2^+$ sandwich and subsequent members would represent the alternating addition of metal–benzene-metal–benzene . . . units. The larger units would then represent multiple-decker metal–benzene sandwiches. The surprising observations first described by Kaya, Nakajima and coworkers have been reproduced in other labs (including ours). The tendency to make these multi-decker sandwiches is less in the late transition metal systems. These species apparently also form clusters with metal cores surrounded by a layer of benzene molecules on their surface in a so-called "rice-ball" structure [50–55].

Because of the unusual and fascinating structures suggested for the multiple-decker metal benzene systems, these clusters have attracted tremendous interest. Several groups have investigated the electronic structure and bonding properties

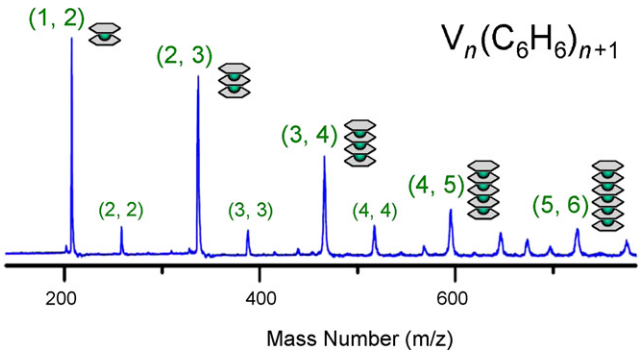

Fig. 2. The mass spectrum of vanadium–benzene complexes containing multiple metal atoms and multiple benzene molecules. The $M_n(benzene)_{n+1}$ stoichiometry pattern suggests that the structures are multiple-decker sandwiches. Figure received from Nakajima, Kaya and coworkers.

of these systems with various forms of ab initio computations, including both ions and neutrals in these studies [55–59]. Bowers and coworkers employed ion mobility methods to the vanadium–benzene systems, which confirmed the multi-decker sandwich structures [60]. The neutral analogues have now been studied by Nakajima, Knickelbein and coworkers with magnetic deflection experiments to investigate the potential magnetism in these species that might arise from spin coupling along the length of the sandwich [61–63]. The stability of these ion and/or neutral species is apparently substantial. The $V(benzene)_2^+$ and $V_2(benzene)_3^+$ cations were mass-selected and deposited into rare gas matrices or organic thin films and the infrared spectra of the corresponding neutral species were measured [64,65].

3. Photodissociation patterns

The mass spectra shown here in Figs. 1 and 2, and in the numerous other studies of metal ion and metal cluster reactions with benzene, indicate that complexes can be formed efficiently, and that certain cluster sizes are more effective in adsorbing benzene. Some circumstantial evidence for cluster structures is provided by stoichiometry in the case of the multi-decker sandwich structures described by Nakajima, Kaya and coworkers. However, mass spectrometry experiments alone do not provide any direct determination of the structures or energetics of these systems. To obtain such insight, additional measurements beyond simple mass spectrometry are required. One of the simplest of these is mass-selected photodissociation, which has been performed in many kinds of mass spectrometer instruments. In some of the early work, Freiser and coworkers used ultraviolet lamp sources to excite ions produced and isolated by mass in a Fourier transform instrument (FT-MS) [66–69]. For the most part, these studies examined mono- or di-benzene complexes, which eliminated intact ligands. The energy dependence of the dissociation yield was used to determine bond dissociation energies, as discussed further below.

Our group has employed laser photodissociation measurements in a specially designed time-of-flight instrument to study some of the larger metal ion–benzene complexes produced by laser vaporization/pulsed nozzle sources [43,70–74]. Fig. 3

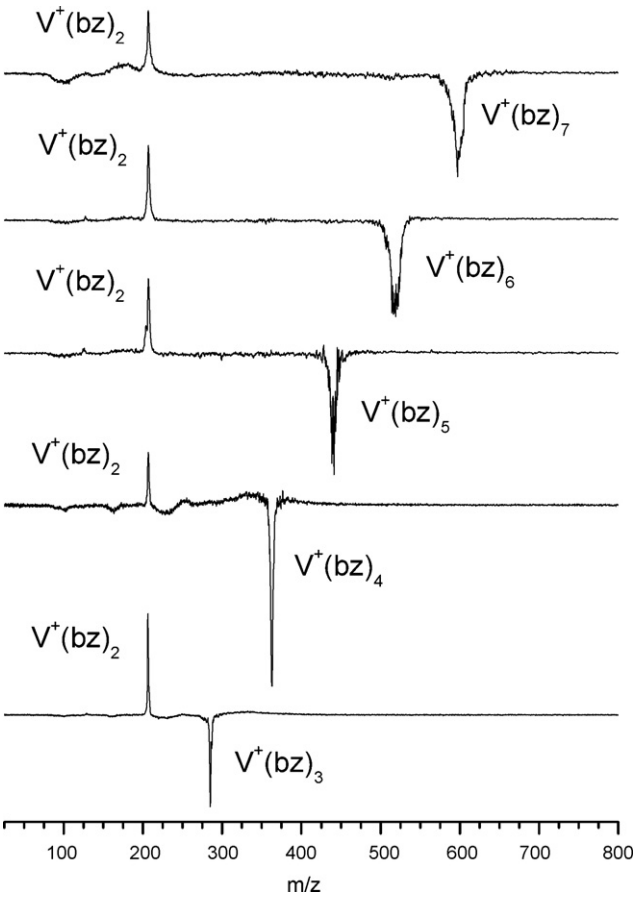

Fig. 3. Photodissociation mass spectra of $V^+(benzene)_n$ complexes for $n = 3$–7. In each case, the $V^+(benzene)_2$ complex is the only photofragment, suggesting that this complex is much more stable than others with more benzenes.

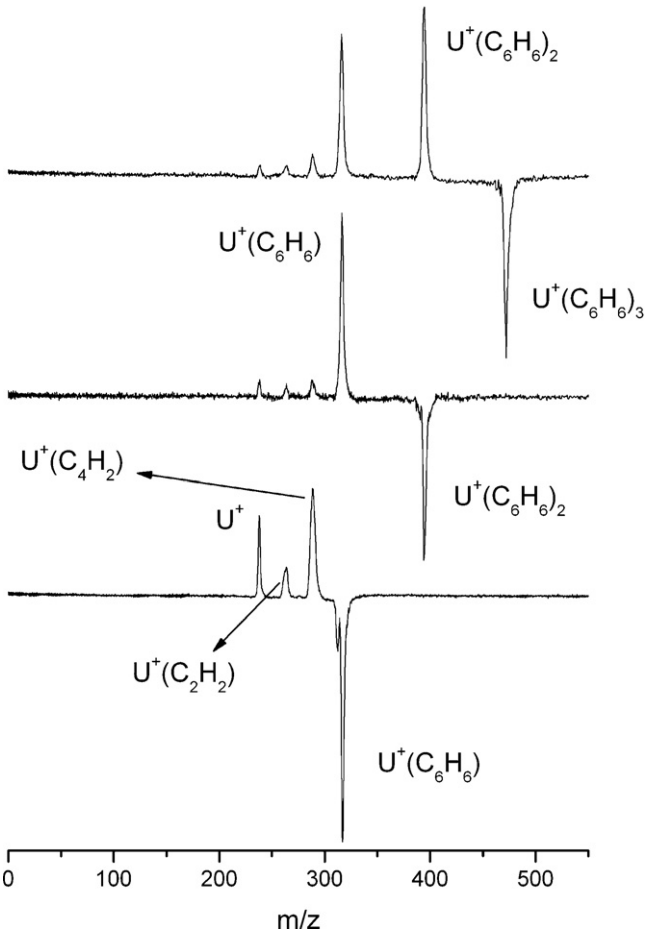

Fig. 4. Photodissociation mass spectra of $U^+(benzene)_n$ complexes for $n = 1$–3. Fragmentation processes disrupt the benzene ligand.

shows an example of this kind of photodissociation experiment for the $V^+(benzene)_n$ complexes ($n = 3$–7) which have been excited with the third harmonic of a Nd:YAG laser (355 nm) [43]. This data and that shown in Figs. 4 and 5 are collected with a computer difference method in which the intensity of the selected parent ion with the fragmentation laser "off" is subtracted from that with it "on." The negative-going signal shows the depletion of the parent ion, and the positive peaks indicate the charged photofragment ions. As shown, each of these complexes eliminates one or more neutral benzene molecules, eventually producing the $n = 2$ complex as the final product. This indicates that the first two benzene ligands are much more strongly bound than subsequent ones, thus unequivocally establishing that the preferred coordination of V^+ is two benzene molecules. Similar experiments have been done on a variety of metal ion–benzene complexes, and also on some metal cluster–benzene systems. Each of the experiments on atomic metal ion complexes finds evidence for a coordination of two benzene ligands.

While most photodissociation experiments detect the elimination of intact benzene molecules, some of these experiments find evidence for photochemical insertion chemistry. Fig. 4 shows an example of this behavior for the uranium–benzene system [70]. In this case, photodissociation not only eliminates intact benzene molecules, but other fragments detected include the metal adduct with C_2 or C_4 hydrocarbon products. Interestingly, in the case of uranium, these products are observed for the bare metal ion complexes, but not for the corresponding uranium oxide ion complexes with benzene. Among the first row transition metals, titanium also exhibits some formation of similar hydrocarbon fragment ions [43]. It is not completely clear in these studies when the dissociation process took place. The mass spectrum in the case of the titanium or uranium systems contained some fragment ions which grew out of the source, as well as the nominally intact $M^+(C_6H_6)_n$ units. However, it is conceivable that some of these ions already fragmented in the growth process, when they interacted with the hot ions resulting from the vaporization process. The laser could then be either eliminating smaller molecules from already-fragmented benzene units, or it could be inducing fragmentation via photochemistry. Unfortunately, photodissociation experiments cannot distinguish between these alternatives. Collisional experiments are better suited to this kind of problem.

Fig. 5 shows another interesting kind of result that may sometimes occur via photodissociation. Most metal ion–benzene complexes photodissociate by losing neutral benzene molecules. This is the expected lowest energy channel for these systems because the metal atom has a lower ionization potential

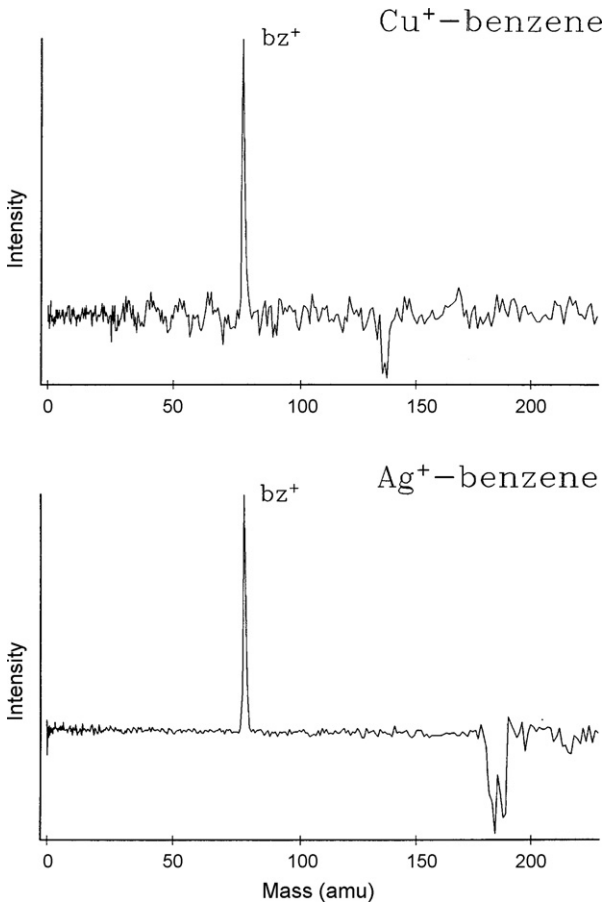

Fig. 5. Photodissociation mass spectra of Cu^+(benzene) and Ag^+(benzene) complexes at 355 nm. Both systems produce the charge transfer product of $C_6H_6^+$ as the only photofragment. The double peak for the silver–benzene parent ion arises from the two naturally occurring isotopes of silver.

(usually 7–8 eV for transition metal atoms) [75] than benzene (IP = 9.24 eV) [75]. However, in certain M^+(benzene) systems, photoexcitation produces the benzene cation (and the neutral metal atom) as the primary dissociation channel, in a charge transfer dissociation process. In many of these systems, collisional dissociation of the same complex produces the expected metal ion and neutral benzene fragments. This indicates that the ground state complex has the charge in the expected position, but that the photoexcitation transfers the charge from the metal atom to the benzene ligand. Fig. 5 shows an example of this kind of behavior, in which the photodissociation of $Ag(benzene)^+$ and $Cu(benzene)^+$ each produces exclusively the benzene cation. Such charge transfer photodissociation has been observed now for a number of metal ion–benzene complexes [71–73]. For transition metal ions that have low-lying excited electronic states (Fe^+, Co^+, Cr^+), excitation of metal ion-based transitions may occur competitive with the charge transfer; the branching ratio between charge transfer and neutral ligand elimination varies with the excitation energy. However, for metal ions like silver and copper, which have virtually no low-lying atomic states that are optically coupled to the ground state via allowed transitions, the charge transfer channel may dominate completely, as shown in the figure [72,73].

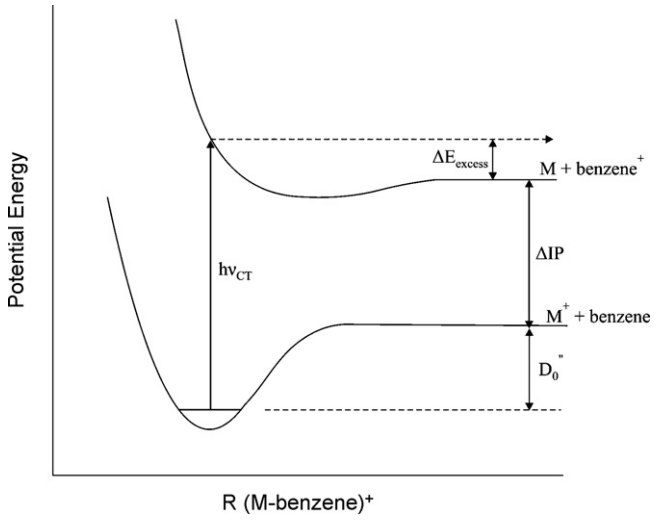

Fig. 6. A schematic diagram of the potential surfaces involved in the charge transfer photodissociation of certain metal ion–benzene complexes (such as that for silver).

Fig. 6 shows a schematic diagram of the electronic states of the metal ion–benzene complex involved in the photodissociative charge transfer process for a metal ion like silver or copper [72,73]. The ground state has the expected character with the charge localized essentially on the metal atom, which has the lower ionization potential. Because silver and copper are closed shell ions, covalent interactions are not strong and the bonding is largely electrostatic in nature. In these systems, the charge-induced dipole electrostatic interaction is especially favorable, because the atomic ion is able to polarize the large benzene molecule. The ground state potential therefore has a significant binding depth. Because the silver or copper ions have no low-lying excited states, the only excited state of the complex is that corresponding asymptotically to the charge-transferred species $M + benzene^+$. The asymptotic energy difference between this and the ground state $M^+ + benzene$ is the ionization potential difference between the metal and that of benzene (1.67 eV in the case of Ag) [72,73]. However, the charge-transfer excited state for species like this is derived from a benzene ion, with a delocalized charge, polarizing a neutral metal atom. This interaction is much weaker than that described for the ground state, and consequently the excited potential minimum is shifted to a longer bonding distance. The Franck–Condon factors in the excitation process for this kind of ion naturally hits the excited state somewhere on its inner wall, and this may well be already above the asymptotic dissociation energy in the excited state, resulting in a direct dissociation process on the excited potential. The fragments corresponding to this excited asymptote are the benzene cation, which is detected, and the neutral metal atom. In principle, an analysis of the kinetic energy of these fragments could be used to determine the excess energy here and in turn to pin down the overall energetics of the system. Because the excitation energy would be known from the dissociation laser wavelength, and the ionization potential difference would also be known, a determination of the excess energy could lead to the M^+-benzene dissociation energy in the ground state, which

are not generally well-known. However, this kind of analysis would have to assume that no internal energy was produced in the benzene moiety, which is not guaranteed. To date, there are many examples of kinetic energy determinations for other kinds of molecules by time-of-flight methods or by photofragment imaging [76,77], but these methods have not been applied to metal–benzene complexes at the time of this writing.

4. Determination of dissociation energies

One of the most fundamental properties of metal ion–benzene complexes is their dissociation energies. In particular, it would be highly desirable to determine the bond energies for mono- and di-benzene complexes of different transition metals and to investigate how these vary for different metal electronic states and spin configurations. Synthetic chemistry can produce complexes efficiently when they have near 18-electron configurations, but metal ion chemistry has virtually no limit on the kinds of complexes that can be produced. Therefore, several different methodologies have been applied over the years to try to determine metal ion–benzene dissociation energies. These methods are described below, and a summary of the values obtained by the different experimental methods is presented in Table 1. The dissociation energy is also readily obtained through ab initio computational chemistry [27–42], and the results of selected theoretical work are also presented in the table for comparison.

Some of the first values for the dissociation energy of metal ion–benzene complexes were reported by Freiser and coworkers [66–69]. Ions were produced either by reactions of volatile organometallic precursors or by laser vaporization followed by association of the metal ions with benzene. Various visible and ultraviolet lamp sources were employed with optical filters for approximate wavelength selection. In this work, the threshold energy at which the fragment ion from a selected metal–benzene or metal–di-benzene complex was first detected was designated as the dissociation threshold. No modeling was done to account for the rate of dissociation following excitation, and how it might vary with energy (see discussion of kinetic shifts below). Additionally, it was inherently assumed by this method that the metal–benzene ions had a continuous absorption spectrum. Ions cannot dissociate unless they first absorb energy into an excited state and then this energy must be transferred efficiently to the ground state via internal conversion. Therefore, the photodissociation threshold energy is actually an upper limit to the ground state dissociation threshold, which is the quantity of interest. However, for many transition metal ions with partially filled valence shells, the density of excited states is high and the thresholds determined in this way by photodissociation do provide a reasonable value for the ground state dissociation energy. The values determined this way for vanadium, iron and cobalt complexes are in reasonable agreement with those obtained by other methods. The situation is much less favorable when the metal ion has no low-lying excited states, as found for the Ag^+(benzene)

Table 1
Binding energies for M(benzene)$_x^+$ ions determined by experiment and theory (kcal/mol). The most likely ground state configuration for the mono-benzene complex is given

	Experiment[a]		Theory		
	$M^+(C_6H_6)$ state	$x=1$	$x=2$	$x=1$[i]	$x=2$[j]
Sc	$^3E_2$ ($3de_2^1 4s^1$)		44.1		
Ti	$^4A_2$ ($3de_2^2 3da_1^1$)	61.8	60.4	62.8, 56.9[j], 54.5[k]	47.4
V	$^5E_1$ ($3de_2^2 3da_1^1 3de_1^1$)	55.8, 62[b]	58.8	51.1, 47.9[j], 47.5[k]	32.2
Cr	$^6A_1$ ($3de_2^2 3da_1^1 3de_1^2$)	40.6, 39.2[c,d]	55.3, 50.7,[c] 49.6[d]	37.4, 38.9[j], 36.4[k]	36.8
Mn	$^7A_1$ ($3de_2^2 3da_1^1 3de_1^2 4s^1$)	31.8	48.4	35.1, 34.5[j], 31.5[k]	29.9
Fe	$^4A_2$ ($3de_2^4 3da_1^1 3de_1^2$)	49.6, 55[b]	44.7	51.1, 56.8[l], 51.5[j], 49.0[k]	40.6
Co	$^3A_2$ ($3de_2^4 3da_1^2 3de_1^2$)	61.1, 68[b]	39.9	62.6, 61.2[j], 58.6[k]	35.9
Ni	$^2E_1$ ($3de_2^4 3da_1^2 3de_1^3$)	58.1	35.1	59.3, 59.9[j], 57.4[k]	33.7
Cu	$^1A_1$ ($3de_2^4 3da_1^2 3de_1^4$)	52.1	37.1	51.1, 51.7[j], 49.1[k]	35.2
Y				40.8, 46.1[m]	
Nb		66[b]		52.1	
Ru		48[b]		48.7	
Ag		37.4,[e] 55[f], 38.7[g]		36.5	
Au		∼70[h]			

[a] Armentrout, Ref. [80], unless otherwise noted.
[b] Freiser, Ref. [23].
[c] Dunbar, Ref. [83].
[d] Baer, Ref. [87].
[e] Armentrout, Ref. [78].
[f] Freiser, Ref. [69].
[g] Ho et al., Ref. [84].
[h] Schwarz, Ref. [86].
[i] Bauschlicher, Ref. [27], unless otherwise noted.
[j] Klippenstein, Ref. [31].
[k] Klippenstein, Ref. [97].
[l] Values are the ^6D and ^4F asymptotes.
[m] Values are the ^1S and ^3D asymptotes.

complex [69]. In this system, the dissociation energy reported by Freiser (55 kcal/mol) was almost a factor of two greater than the values determined by other groups (e.g., 37.4 kcal/mol by Armentrout [78]). The source of this discrepancy is undoubtedly that Ag^+(benzene) does not absorb light efficiently anywhere near the energy of its ground state dissociation energy.

The appearance of photodissociation at an excited state charge-transfer threshold can also be used to determine an upper limit on the ground state dissociation energy. As shown in our work on Ag^+(benzene), this can be done using the threshold for the appearance of the charge transfer channel producing the benzene cation photofragment. As shown in Fig. 6, the excited state charge-transfer threshold energy should be found when the photon energy used for excitation ($h\nu_{CT}$) equals the combined energy of the ground state dissociation energy ($D_{0''}$) plus the ionization potential difference between the metal ion and the benzene molecule (ΔIP). The limit on the ground state dissociation energy is then simply given by the difference $D_{0''} \leq h\nu_{CT} - \Delta IP$. If the Franck–Condon factors in the photoexcitation process allow efficient excitation at the actual threshold, the true ground state dissociation threshold can be obtained in this way. Fig. 7 shows the excitation spectrum for Ag^+(benzene) in which the wavelength dependence was recorded for the benzene cation channel [72]. Neither benzene itself nor the silver cation have any low energy excited states, but the complex actually absorbs light down into the blue visible region of the spectrum. The onset measured at 418 nm leads to a derived upper limit on the ground state dissociation energy of 30.0 kcal/mol. This value is significantly lower than the value reported by Freiser using the onset of the Ag^+ + benzene photodissociation channel [69]. Surprisingly, this lower limit value is also lower than the collision induced dissociation value determined by Armentrout (37.4 kcal/mol [78]). It is not at all clear what causes this discrepancy. However, if the ions in our experiment were internally hot or if there were multiple photon absorption events, the threshold derived in our experiment could be lower than the real value. Because these effects are difficult to exclude completely, we believe that the dissociation energy determined by Armentrout is probably more accurate.

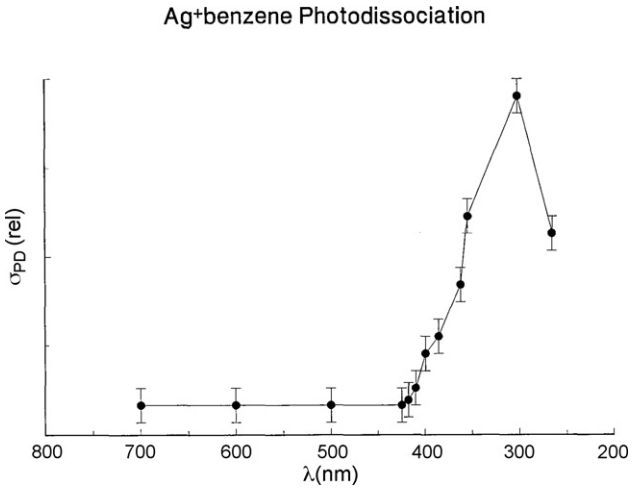

Fig. 7. The photodissociation action spectrum of the Ag^+(benzene) complex showing the wavelength dependence of the $C_6H_6^+$ product ion.

Perhaps the most widely applied method for the determination of bond energies is energy variable collision induced dissociation (CID). In this method, which has been applied to many transition metal ion–molecule complexes by Armentrout and coworkers [78–81], the metal ion complex of interest is produced and size-selected, and then the ion beam kinetic energy is adjusted prior to guiding the beam into a collision cell which is filled with a rare gas. Experience has shown that heavier rare gases (krypton, xenon) are more effective at energy transferring collisions. The pressure must be adjusted to ensure that only a single collision takes place for each ion as it passes through the collision cell, and the lab frame kinetic energy must be converted into the center-of-mass frame. Additionally, it is found that dissociation following such collisions take place within the normal framework of unimolecular dissociation theory. Because energy can be randomized over the available internal degrees of freedom of the ion–molecule complex, the rate of bond breaking depends on the density of vibrational states and the amount of internal energy deposited and how it compares to the energy threshold for bond breaking. In practice, the dissociation yield for larger molecules such as metal ion–benzene complexes is low at threshold and rises up to a measurable value only at an energy somewhat above threshold. This so-called kinetic shift in the threshold, and the rate of dissociation as a function of energy, can be analyzed with various forms of transition state or phase space methods to pin down the exact dissociation threshold energy. The required input is a set of vibrational frequencies for the complex, which are not generally known. However, vibrational frequencies from theory are usually acceptable for this analysis, as the unimolecular rate is less sensitive to these frequencies than it is to the dissociation threshold. Because of the need for vibrational frequencies in the data analysis, CID studies are often accompanied by ab initio or density functional theory calculations. The Armentrout group has been a leader in the measurement of CID thresholds and in the development of methods for the analysis of the threshold data. A number of dissociation energies for metal ion–benzene and metal ion–di-benzene complexes determined by this group are presented in Table 1, where they are compared to the results of other experiments and to the predictions of theory. As shown, these bond energies vary over the range of 30–60 kcal/mol for different metals.

Another method for the determination of metal ion–benzene dissociation energies is the analysis of radiative association kinetics. If a metal ion and a benzene molecule are brought together in vacuum, they can form an association complex, which may simply re-dissociate or it may become stabilized via the emission of infrared light (i.e., heat). The kinetic scheme for this system is

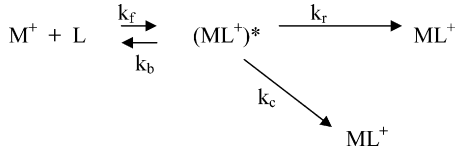

where k_f and k_b are the rates of complex formation and back dissociation, k_r is the rate of IR radiative stabilization of the

complex, and k_c is the rate of collisional stabilization of the complex. If the pressure is low, k_c is negligible. Studies as a function of pressure can be used to obtain the low-pressure limit. The radiative rates can be determined from an ab initio calculation of the vibrational frequencies and infrared oscillator strengths of the vibrations. Finally, the reverse rate of dissociation of the complex depends in a very sensitive way on its internal energy relative to the dissociation energy of the bond which breaks. Variational transition state theory can be employed to calculate the rate constants in this system, where the variable parameter used to fit the rates is the dissociation energy. This methodology has been described in detail by Dunbar [82]. A number of metal ion–benzene systems have been studied using radiative association by Dunbar and coworkers and by Schwarz and coworkers [83–86]. The Au^+(benzene) complex has attracted special attention in this regard, because the ionization energies of benzene (9.244 eV) [75] and gold (9.226 eV) [75] are essentially the same. The charge exchange channel therefore adds additional complexity to the kinetic modeling for this system.

Li and Baer have employed the threshold photoelectron-photoion coincidence method (TPEPICO) to investigate the dissociation energies of $Cr^+(benzene)_{1,2}$ [87]. This method, which models the experimental product ion time-of-flight distribution, makes it possible to identify the initial ionization threshold and higher fragmentation thresholds with high accuracy, thus allowing the metal ion-ligand bond breaking energy to be extracted. This methodology has been employed extensively in non-metal ion chemistry, but it has not been applied to many metal ion–benzene complexes.

As can be seen from the entries in Table 1, the bond energies of these metal ion–benzene complexes are substantial, and they vary significantly with different transition metals. The bond energy for Ti^+(benzene) (61.8 kcal/mol) is among the highest values for the mono-benzene complexes of the first-row transition metals, and then the values for V^+, Cr^+ and Mn^+ complexes are gradually lower. Mn^+ has the lowest bond energy of the first row species. After Mn^+, the bond energies increase, with Co^+ and Ni^+ having values about the same as Ti^+ and V^+, and then the value for Cu^+ is somewhat lower again. The di-benzene complexes have bond energies for the second ligand comparable to those of the first, with the values falling off gradually across the period. The noble metal ions, with nominally filled d shells, have relatively lower bonding energies than those for the open shell species, except for the case of Au^+, where the binding energy is believed to be quite high.

It is interesting to consider the electronic structure patterns of bonding stability suggested by these dissociation energies. The stability of sandwich complexes like ferrocene and di-benzene chromium is usually associated with the 18-electron rule. However, all metal cation mono-benzene complexes and most di-benzene complexes ($Mn^+(benzene)_2$ is the only exception) do not have 18 electrons, but these systems exhibit significant bonding stability. As described by Bauschlicher [27] and others since, the bonding in these ionized complexes represents a composite of electrostatic (charge-induced dipole) and covalent interactions. Because of the d contraction, the size of transition metal cations generally decreases across the period, and this reduced

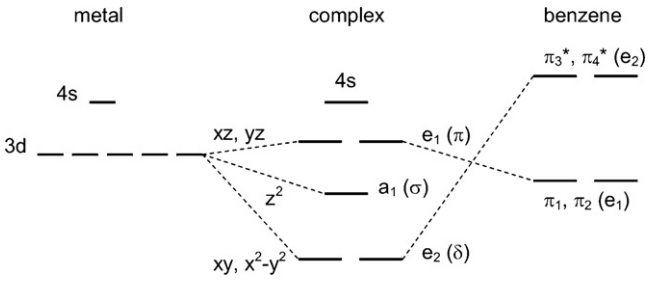

Fig. 8. Schematic molecular orbital diagram for mono-benzene complexes with transition metal cations.

volume enhances the electrostatic component because the metal ion more closely approximates a point charge. The covalent character depends on the details of the bonding orbitals of the complex and their occupation. Although structural variations are expected in some of these complexes (see below), it is convenient for the sake of bonding comparisons to assume symmetric structures for the mono-benzene complexes. In C_{6v} symmetry, the outermost metal 3d orbitals of a M^+(benzene) complex are in the energetic order of $3de_2(\delta) < 3da_1(\sigma) < 3de_1(\pi)$ [27]. A schematic diagram showing the molecular orbitals for a mono-benzene complex like this is shown in Fig. 8. Occupation of the $3de_2(\delta)$ orbitals causes back-donation into the π^* orbitals on benzene and strengthens the metal-ligand bonding, while the $3de_1(\pi)$ orbitals overlaps with the benzene π orbitals and are antibonding. The $3da_1(\sigma)$ orbital points to the center of the benzene ring and its overlap with the benzene orbitals is small. The $3de_2(\delta)$ orbitals are filled in all the metal ion–benzene complexes. Therefore, we can focus on the occupation of the $3de_1(\pi)$ orbital to explain at least some of the trends in the bonding. If we do this, then the decreasing bond energy for the $Ti^+ \rightarrow V^+ \rightarrow Cr^+$ complexes can be attributed to the 3, 4, and 5 electrons, respectively in the $3de_1(\pi)$ orbital. Likewise, the decrease in bond energy for the $Co^+ \rightarrow Ni^+ \rightarrow Cu^+$ series can be associated with the 8, 9, and 10 electrons in this orbital. The Mn^+ complex has the lowest bond energy of the first-row complexes, suggesting that occupation of the 4s orbital is also unfavorable, presumably because of the increased ligand repulsion. On the other hand, the increase in bond energy on going from the Cr^+ complex to the Fe^+ system can be attributed to the addition of a bonding electron to the $3de_2(\delta)$ orbital. The di-benzene complexes exhibit a smooth decrease in bond energies across the period. Surprisingly, the 18-electron species $Mn^+(benzene)_2$ falls in this smooth trend and has no obvious "extra" stability. Additional subtleties come into play in the bond energies depending on structural variations from C_{6v} or D_{6h} symmetries and depending on whether high-spin versus low spin electronic states are preferred, as discussed in many previous theoretical studies [27,31,97].

5. Electronic spectroscopy

As shown above in the discussion of bond energies, any discussion of transition metal ion–benzene complexes eventually turns to questions of structures and electronic configurations, which can only be probed directly with spectroscopy. Unfortunately, as is well-known in the ion chemistry community, the

spectroscopy of ions is quite challenging because of the low densities produced, and the density becomes even lower after mass-selection. Because none of the ion sources used for this kind of work can produce only one species, mass selection is absolutely essential for well-defined experiments. Progress in the spectroscopy of metal ion–benzene complexes is therefore much more limited than in other experimental studies on these ions. To our knowledge, there are no examples yet of direct absorption or laser induced fluorescence measurements on these systems. Instead, the spectroscopy to date has involved photoelectron and mass-selected photodissociation measurements.

In some of the earliest work, Kaya and coworkers probed their multiple-decker sandwich systems of vanadium with anion photoelectron spectroscopy (PES) [88]. In this measurement, a negative ion complex is mass-selected and photo-excited with a fixed-frequency laser whose energy exceeds the electron affinity of that complex. Because of the pulsed ion source employed, pulsed lasers (Nd:YAG laser harmonics at 532 and 355 nm) were used for these experiments. Electron kinetic energy analysis was accomplished with a magnetic-bottle time-of-flight photoelectron spectrometer. More recently, Bowen and coworkers have applied similar methods to mono- and di-benzene complexes of cobalt, nickel and titanium [89–91]. In all of these PES studies, the structure in the spectrum is associated with specific electronic transitions; vibrational structure is not usually resolved. Moreover, the main information about state splittings, etc., is for the *neutral* metal–benzene species, which is the final state populated after photodetachment. Nevertheless, the specific electron affinity value obtained and the Franck–Condon profiles of the electronic states allow information to be obtained about the electronic states involved. For example, Bowen and coworkers concluded that $Cr(benzene)_2^-$ (electron affinity = 1.31 eV) has a symmetric sandwich structure with a singlet ground state configuration [89]. Electron affinities for other transition metal complexes are given in Table 2.

Higher resolution information can be obtained in photoelectron spectroscopy using the pulsed field ionization-zero electron kinetic energy (PFI-ZEKE) photoelectron spectroscopy method [92]. Yang and coworkers have applied this methodology to a number of cation–molecular complexes, including metal–benzene systems [93–95]. This experiment begins with the neutral metal–benzene complex which is excited near its ionization threshold with a tunable ultraviolet laser such as a dye laser. High energy Rydberg states lying within a cm^{-1} or so of the ionization threshold are produced by the optical excitation, and field ionized by a small voltage pulse. Spectra are recorded by measuring the yield of the near-zero energy electrons that are produced at this threshold and for those corresponding to other electronic and/or vibrational resonances that occur above this initial threshold. The resolution of this technique depends on the laser bandwidth and the voltage pulse amplitude, but not on the energy resolution of devices used to analyze the electron kinetic energies. Any shifts in peak positions induced by the pulsed-field sampling method can be corrected for by a systematic study of the voltage dependence of the bands. In this way, PFI-ZEKE spectra provide a highly accurate determination of the ionization potential and a measurement of vibrational structure in the corresponding metal cation–benzene ground state. Mass selection is also obtained in the sense that different complexes usually have different ionization potentials. The threshold signal can be measured with a time-of-flight mass spectrometer, thus identifying the ion, and then the threshold electron spectrum can be measured at this same energy. (The experimental configuration for PFI-ZEKE is easy to incorporate into a time-of-flight mass spectrometer.) Small clusters (mono-benzene versus di-benzene) can usually be distinguished in this way, but this method is less discriminating for larger clusters with similar ionization potentials. An example of PFI-ZEKE spectra obtained for the scandium benzene and scandium di-benzene complexes is shown in Fig. 9.

Several aspects of the PFI-ZEKE experiment as it is implemented for metal–benzene complexes are worth noting. Although the ionization potentials of many transition metal atoms are in the range of 6–9 eV [75] and the ionization potential of benzene itself is 9.24 eV [75], the ionization potentials of metal–benzene complexes are often found to be much lower than this, as shown in Table 2. Because the ionization potential of the metal is lower than that of benzene, the electron removed upon ionization can be viewed to come from the metal atom, and the charge in the complex will be localized on the metal atom. Because the cation–benzene complex has both covalent and electrostatic components in its bonding and the corresponding neutral complex has only the covalent contribution, cation–benzene complexes are usually more strongly bound than their corresponding neutrals. The potentials and energy levels for the ionization process then are inverted with respect to those shown in Fig. 6. The ground state is more weakly bound and the excited state (the ion) is more strongly bound with a deeper well. The transition from the ground state of the neutral complex to that of the cation complex is then at lower energy than the asymptotic transition for the metal atom. This is the origin of the lower ionization potential for the complex. Closely related to this is the vibrational activity that accompanies ionization. Again, because the electron is essentially removed from the metal atom, there is a significant change in the metal–ligand

Table 2
Ionization potentials and electron affinities for selected transition metals [75] and their benzene complexes (eV)

Metal	M		M(benzene)		$M(benzene)_2$	
	IP	EA	IP	EA	IP	EA
Sc	6.54	0.188	5.158[a]		5.069[a]	
Ti	6.82	0.079		0.85[b]	5.732[c]	0.18[b]
V	6.74	0.525		0.62[d]	5.784[c]	neg.[d]
Cr	6.77	0.666			5.465[e]	
Co	7.86	0.662				0.5[f]
Mo	7.10	0.748			5.527[e]	
W	7.98	0.815			5.410[e]	

For comparison, the IP of benzene is 9.24 eV [75].
[a] Ref. [93].
[b] Ref. [91].
[c] Ref. [95].
[d] Ref. [88].
[e] Ref. [94].
[f] Ref. [89].

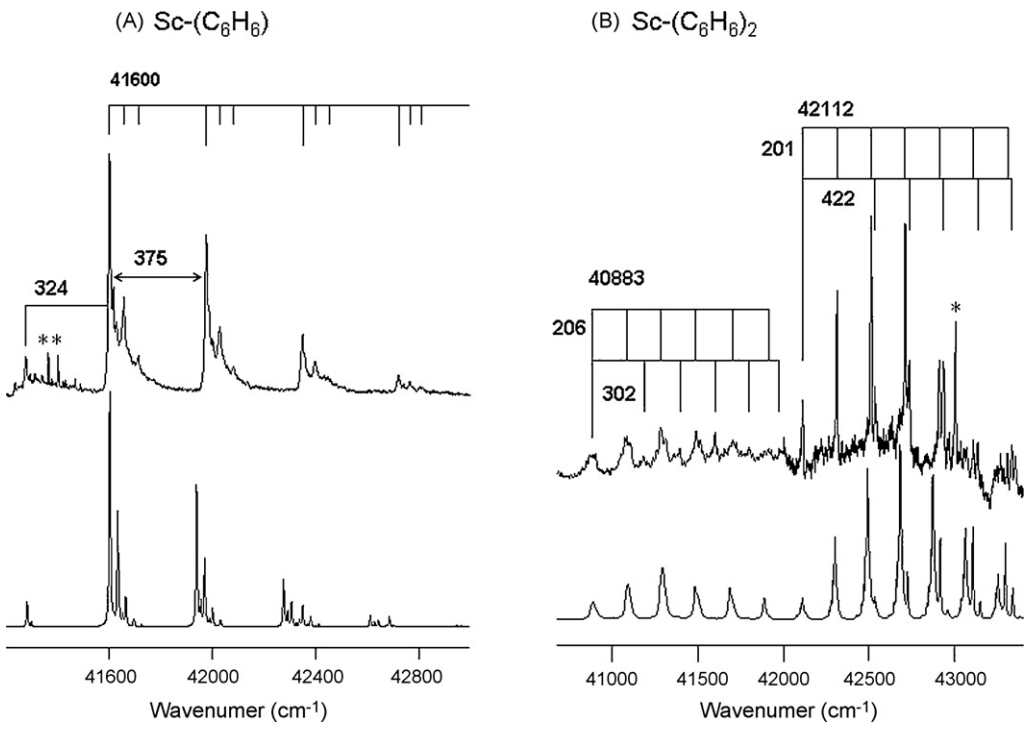

Fig. 9. Experimental ZEKE spectra (top) and simulations (bottom) of $Sc(C_6H_6)$ (A) and $Sc–(C_6H_6)_2$ (B). The simulation of $Sc(C_6H_6)$ is for the $^3A_1 \leftarrow {}^4A_1$ transition, whereas the simulations of $Sc(C_6H_6)_2$ are for the $^1A_g \leftarrow {}^2B_{3g}$ (lower energy) and $^3A_{1g} \leftarrow {}^2B_{3g}$ (higher energy) transitions. Figure received from Prof. Dong-Sheng Yang.

bond distance between the neutral ground state and the cation final state. This provides the greatest Franck–Condon activity in the metal–ligand stretch coordinate. This stretch for most transition metal ion complexes with benzene lies in the 200–400 cm^{-1} region (see progressions in Fig. 9), and this is generally too low in frequency for infrared laser experiments. PFI-ZEKE is therefore the only method presently available to detect these low frequency vibrations. Other totally symmetric vibrations that might couple to the metal–benzene stretch may also be active in the ZEKE spectrum. This means that the vibrations detected in this experiment may have quite different symmetries from those detected by infrared spectroscopy (see below), and indeed PFI-ZEKE and IR spectroscopy complement each other quite nicely.

A final variety of electronic spectroscopy that has been applied to metal cation–benzene complexes is electronic photodissociation. In this method, the cation is produced in a cluster ion source, mass-selected and photo-excited with a visible or ultraviolet laser such as a dye laser or an optical parametric oscillator (OPO). If fragmentation occurs, the fragment ion can be detected and recorded as a function of the excitation energy to record a spectrum. Because the mass spectrometer is the detector, and essentially all fragment ions can be collected and recorded, this method is far more sensitive than simple absorption spectroscopy and also much more sensitive than laser induced fluorescence. Fig. 7, which was discussed earlier, shows an example of the electronic photodissociation spectrum of Ag^+(benzene) [72]. In such a photodissociation spectrum, the excited states probed by the excitation can be derived from the states of the metal ion or its ligand, or there may be a charge-transfer transition, as shown in Fig. 7. Unfortunately, because transition metal ions have ionization potentials in the 6–8 eV range and the IP of benzene is 9.24 eV [75], the IP difference between the two often falls in the range of 2–3 eV, which corresponds to the middle of the visible spectrum. Thus, most transition metal ion–benzene complexes are expected to have charge-transfer electronic transitions like that shown in Fig. 7. The Franck–Condon considerations discussed above for these kinds of transitions usually lead to intense broad resonances, which would therefore overlap and obscure any other discrete electronic transitions for these species. To a large degree because of this, no sharp spectra (vibrationally resolved) have been obtained for transition metal ion–benzene complexes via this kind of electronic photodissociation spectroscopy.

6. Infrared spectroscopy

Infrared spectroscopy is one of the most common tools for molecular structural analysis, and it is therefore expected to be extremely important for the determination of the structures and bonding configurations of metal ion–benzene complexes. However, IR spectroscopy suffers from all the same difficulties that electronic spectroscopy does. The density of mass-selected ions is too low for absorption spectroscopy, and so some sort of action spectroscopy is required. Infrared photodissociation spectroscopy has become the method of choice for these experiments, but there are some serious caveats in its implementation.

The most obvious problem with infrared photodissociation spectroscopy involves the energetics of this experiment. In the photodissociation method, absorption of light is detected by

the breaking of a bond that occurs after absorption. Hence, fragmentation provides the evidence of absorption at a specific wavelength. However, the ability to break bonds with light depends on the specific energies of the bonds that are to be broken compared to the photon energy employed. As noted in Table 1, the bond energies of metal cation–benzene complexes are in the range of 30–60 kcal/mol, which corresponds to 24,000–48,000 cm^{-1}. Visible or near-UV light therefore has enough energy to break these bonds, explaining the success of UV–vis laser photodissociation, as described above. However, infrared excitation necessarily involves photon energies corresponding to vibrational fundamentals, and the highest frequencies for metal ion–benzene complexes are those of the C–H stretches, which occur near 3000 cm^{-1}. Infrared excitation at this energy is far below the threshold for bond-breaking, and therefore "simple" photodissociation experiments with infrared light are not possible.

Two general approaches have been successful in overcoming the energetics of infrared photodissociation. If high intensity light sources are available, resonance-enhanced infrared multiple photon photodissociation (IR-REMPD) can be achieved. In this method, the first photon is absorbed on a vibrational fundamental, and then additional photons are absorbed rapidly following this until the sum of the multiple photon energies is able to accomplish dissociation. IR-MPD has been applied to neutral molecules beginning with the advent of high-power pulsed CO_2 lasers almost 30 years ago, and its mechanism has been studied extensively [96]. This methodology was first applied to mass-selected ions by Beauchamp and coworkers [97], but it has been employed extensively in ion chemistry over the years [98]. In the case of metal ion–benzene complexes, the dissociation energies indicated above require the absorption of at least 8–10 photons to reach the dissociation threshold. Unimolecular dissociation then proceeds at a rate dictated by intramolecular energy redistribution (IVR) and the amount of excess energy, as has also been well studied [99]. In spectroscopy measured with IR-REMPD, high laser pulse energies are therefore required to accomplish efficient dissociation on a fast enough time scale for detection, but the pulse energy must be low enough so that off-resonant absorption is not too efficient, thus allowing resonances to be detected. In the delicate intermediate pulse energy range, resonances may be power broadened, and they may be shifted toward lower energies than the actual fundamental absorption frequencies because of the effects of an harmonicity in the multiple photon process [96,100,101]. In a collaboration with the group of Meijer and coworkers, our research group has performed IR-REMPD spectroscopy on a number of mono- and di-benzene complexes of the first row transition metals [102,103] using the tunable free electron laser known as FELIX [100]. Some of the spectra resulting from these studies are presented in Figs. 10–12.

A second way to deal with the dissociation energy problem in IR photodissociation is the method of "inert gas tagging" [104–108]. In this method, a weakly bound rare gas atom (argon, neon) or small molecule (hydrogen, nitrogen) is added to the ion of interest as a leaving group to enhance the efficiency of photodissociation. The mixed complex, e.g., M^+(benzene)Ar, is

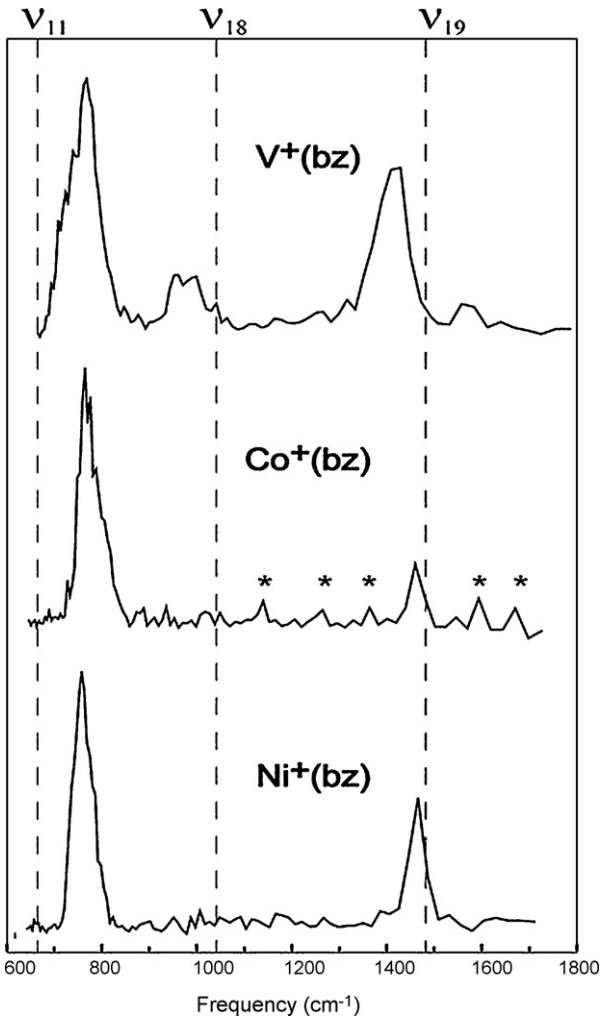

Fig. 10. The IR-REMPD spectra measured for the vanadium, cobalt and nickel cation mono-benzene complexes using the FELIX free electron laser. The peaks marked with an asterisk are from electrical noise and not caused by true ion signals. The dashed lines indicate the position of free benzene vibrations.

mass-selected and, because the argon tag atom bonding energy is relatively low, infrared excitation of this complex leads to efficient elimination of the argon. The technique works well when the tag binding is small. This is not always true for argon, whose binding energy with some transition metal ions can be 2500–3000 cm^{-1}. In these cases, tagging with a more weakly bound species such as neon would be preferred. The tagging method also requires that the indicator atom or molecule not perturb the spectroscopy too much. To make sure that this is the case, it is typical to apply computational methods to both the isolated ion and its tagged counterpart. Predictions of the infrared spectra with and without the tag can be used to determine the perturbation, if any. In many cases, we have found that shifts in vibrations caused by tagging range from 1 to 2 cm^{-1} in favorable cases up to about 10 cm^{-1} in the worst cases. The exception to this occurs for argon tagging of protonated molecular species, in which the argon binds directly to the proton. In these cases, the proton stretch vibration is highly perturbed and may shift by 100 cm^{-1} or more [106]. Our lab has pioneered the study of transition metal ion complexes using the tagging method [108].

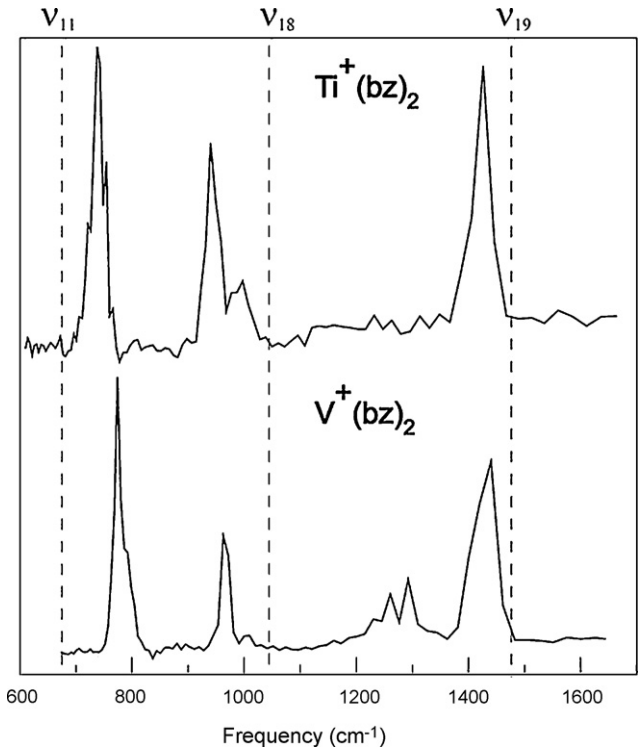

Fig. 11. The IR-REMPD spectra measured for the titanium and vanadium cation di-benzene complexes using the FELIX free electron laser. The dashed lines indicate the position of free benzene vibrations.

Figs. 13–16 show examples of vanadium and nickel ion–benzene complexes studied in this way [109,110].

Another serious problem with infrared photodissociation spectroscopy has been the limited availability of broadly tunable, high intensity infrared laser sources. Until recently, laboratory-based pulsed infrared light with enough intensity to study pulsed ion beams was only available from optical parametric oscillators (OPO's) using lithium niobate crystals or from dye laser difference frequency generation in these same crystals. Both of these methods provided light in the 2700–4000 cm^{-1} region with reasonably good intensity. Beginning about 5–7 years ago, new OPO systems became available using potassium titanyl phosphate (KTP) and arsenate (KTA) crystals, making it possible to expand the coverage of the OPO sources down to about 2000 cm^{-1} on the lower frequency end [111]. Our group has used these KTP/KTA OPO systems to study several metal ion–benzene complexes with argon tagging, as shown in Figs. 13–16 [109,110]. Unfortunately, the KTP/KTA OPO systems still do not provide coverage of the fingerprint region of the infrared, where the most distinctive structurally dependent patterns are to be expected. The solution to this problem has been to obtain tunable IR light at lower frequencies from free-electron lasers (FEL's) such as those available at the F.O.M. Laboratory for PlasmaPhysics in Rijnhuisen, The Netherlands (known as FELIX), or at the Centre Laser Infrarouge d'Orsay (CLIO) in Orsay, France. These FEL laser sources provide coverage of the 400–2000 cm^{-1} region and with some modifications can also work at higher frequencies. The disadvantage of these systems is of course their limited access compared to benchtop

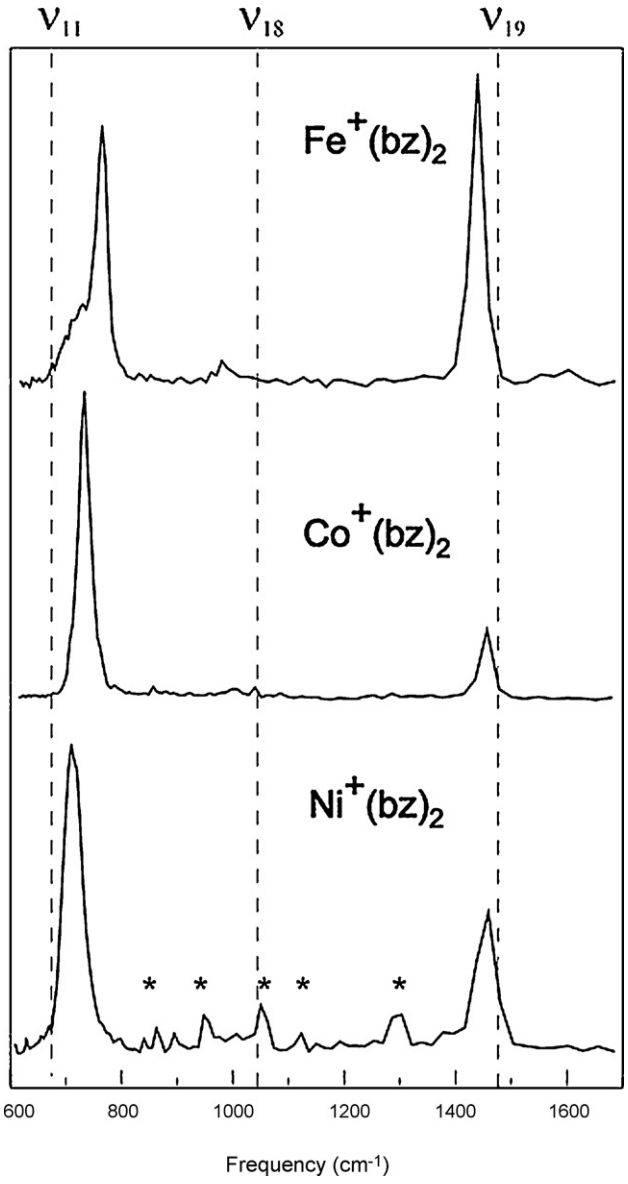

Fig. 12. The IR-REMPD spectra measured for the iron, cobalt and nickel cation di-benzene complexes using the FELIX free electron laser. The peaks marked with an asterisk are from electrical noise and not caused by true ion signals. The dashed lines indicate the position of free benzene vibrations.

IR systems. As mentioned above, our group, in collaboration with Meijer and coworkers, used the FELIX FEL to measure IR-REMPD spectroscopy in the fingerprint region for several metal ion–benzene complexes, as shown in Figs. 10–12 [102,103]. A final advance in IR-OPO systems has occurred in just the last two years or so. New silver gallium selenide ($AgGaSe_2$) and lithium thiol indate (LiS_2In_2) crystals now provide coverage over the 600–2000 cm^{-1} region, completing the spectral coverage of the KTP/KTA OPO systems [112]. Many new IR spectroscopy experiments on ions have been described using these systems, but this new capability has not yet been applied to metal ion–benzene complexes.

Although the infrared measurements on metal ion–benzene complexes have been somewhat limited by all the experimental difficulties, some significant insight has been possible from

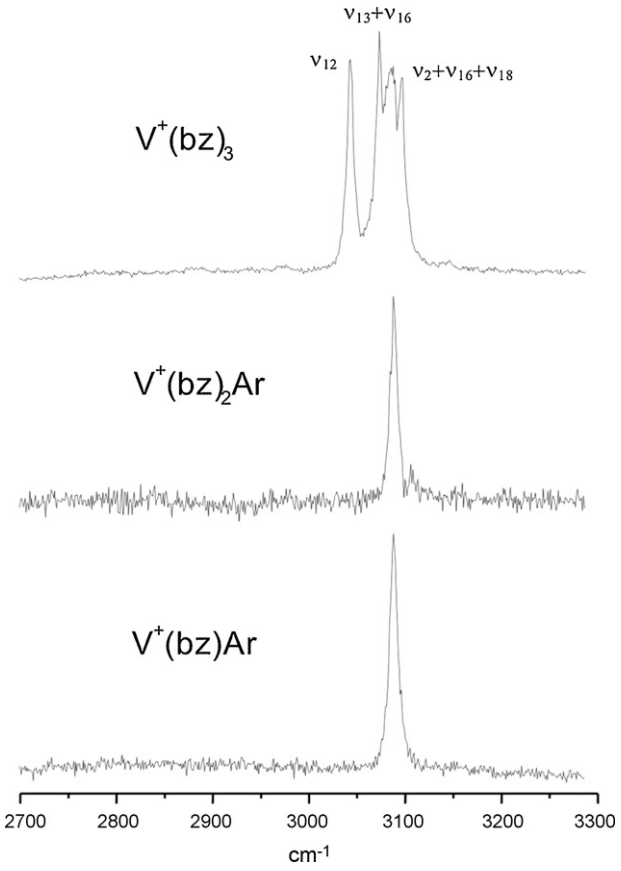

Fig. 13. The infrared photodissociation spectra of the V^+(benzene)Ar, V^+(benzene)$_2$Ar and V^+(benzene)$_3$ measured in the loss of argon channel (for the mono- and di-benzene species) and the loss of benzene channel (for the tri-benzene species).

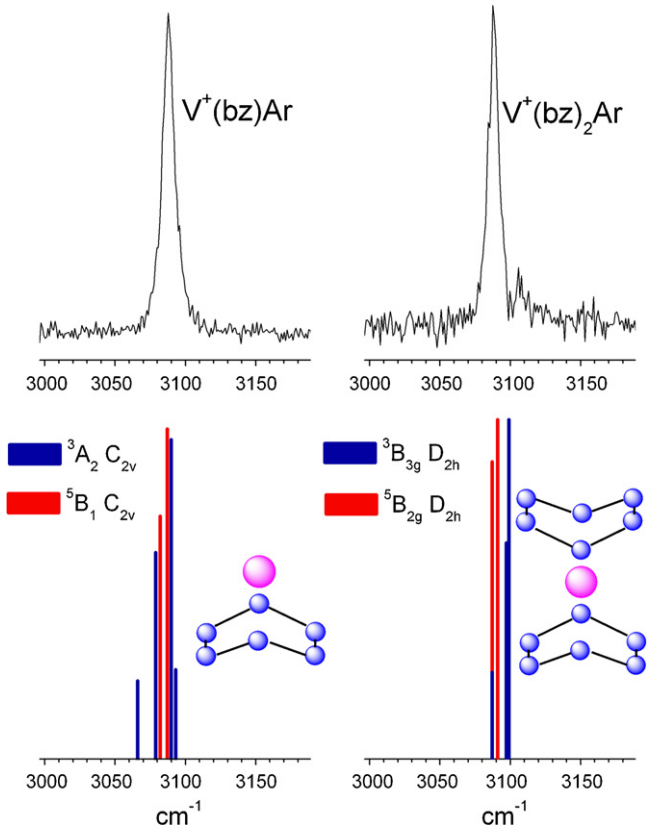

Fig. 14. The infrared photodissociation spectra of the V^+(benzene)Ar and V^+(benzene)$_2$Ar complexes in the argon elimination channel compared to the predictions of theory for the IR absorption spectra for these complexes. The blue versus red band positions from theory correspond to the spectra for the triplet versus quintet ground states. In both cases the quintet spectra exhibit better agreement with the observed spectra (For interpretation of the references to color in this figure legend, the reader is referred to the web version of the article.).

the experiments done so far. Figs. 10–12 show the IR-REMPD spectra that we have measured in our collaboration with Meijer and coworkers using the FELIX free-electron laser [103]. For these experiments, the ions were produced by photoionization of the corresponding neutrals, and mass-selected using an ion trap/time-of-flight instrument. Multiple photon photodissociation resulted in the elimination of benzene from the selected parent ion, and the fragment ion intensity was recorded versus the IR wavelength. Several vibrational spectra in the fingerprint region were obtained for mono- and di-benzene complexes.

Fig. 10 shows the IR-REMPD spectra for the mono-benzene complexes of vanadium, cobalt and nickel cations. As indicated, all three have resonances in the 600–1700 cm^{-1} region. The dashed vertical lines at 673, 1038 and 1486 cm^{-1} mark the positions of the main IR-active vibrational bands of the gas phase benzene molecule [113]. They are respectively the ν_{11} (out-of-plane C–H bend), ν_{18} (in-plane C–H bend) and ν_{19} (in-plane carbon ring distortion) vibrational modes. Strong resonances in the IR-REMPD spectra occur for all three complexes near the ν_{11} and ν_{19} bands in benzene, and a weaker band in the vanadium complex occurs near the ν_{18} band in benzene. Figs. 11 and 12 show similar IR-REMPD spectra for the di-benzene complexes of titanium, vanadium, iron, cobalt and nickel. These spectra are qualitatively similar to the mono-benzene complexes, with strong resonances seen near the ν_{11} and ν_{19} vibrations for all five metal complexes. The titanium and vanadium complexes have additional structure near the ν_{18} band, but this region of the spectrum has little or no intensity for the iron, cobalt and nickel complexes.

It is evident from Figs. 10–12 that all of these complexes have vibrational bands near those of the free benzene molecule. The bands near 730–770 cm^{-1} all occur at higher frequency than the ν_{11} (a_{2u}) out-of-plane C–H bend in benzene at 673 cm^{-1}. The bands in the 900–1000 cm^{-1} region are not seen for all complexes, but they generally appear at frequencies lower than that of the ν_{18} (e_{1u}) in-plane C–H bend at 1038 cm^{-1}. Strong bands are also seen in the 1420–1470 cm^{-1} region, and these generally lie at lower frequency than the ν_{19} (e_{1u}) carbon ring deformation mode that occurs at 1486 cm^{-1} in benzene. Vibrational patterns similar to these have been seen and discussed previously for a variety of condensed phase metal di-benzene complexes produced by conventional synthetic chemistry [10,12,18]. These systems are usually studied in solution or in thin solid films, and therefore vibration band positions are not generally known for the isolated molecules. However, the vibrational assignments and their trends provide a convenient guide for our work.

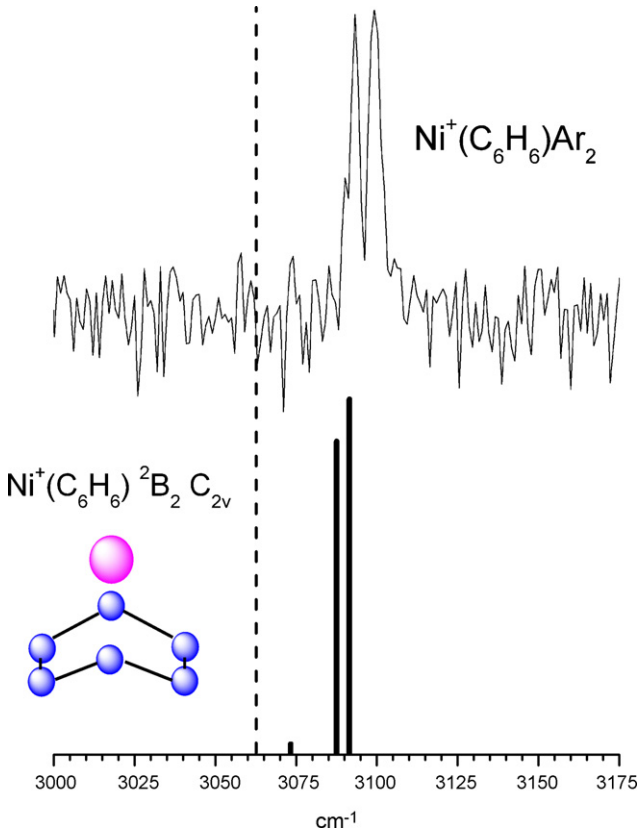

Fig. 15. The infrared photodissociation spectra of the $Ni^+(benzene)Ar_2$ complex in the argon elimination channel compared to the prediction of theory for the IR absorption spectrum for this complex in the C_{2v} structure shown. The dashed line indicates the position calculated for the ν_{12} vibration in free benzene in the absence of the Fermi resonance.

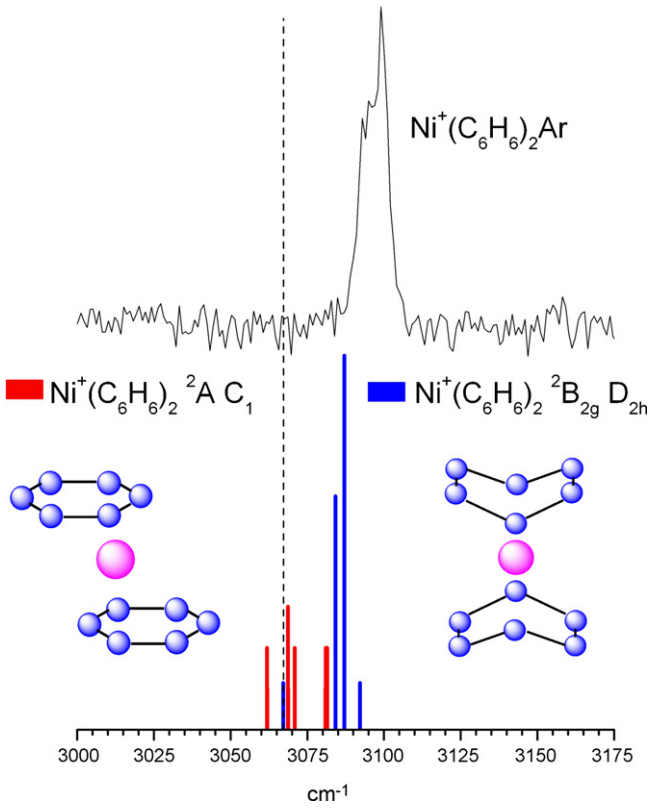

Fig. 16. The infrared photodissociation spectra of the $Ni^+(benzene)_2Ar$ complex in the argon elimination channel compared to the prediction of theory for the IR absorption spectrum for this complex in the C_1 versus D_{2h} structures shown. The spectrum predicted for the D_{2h} structure matches the experiment better, even though this is not the lowest energy structure predicted by density functional theory. The dashed line indicates the position calculated for the ν_{12} vibration in free benzene in the absence of the Fermi resonance.

In the IR spectra of condensed phase metal–benzene complexes, the ν_{11} and ν_{19} bands are prominent. The ν_{11} band is usually shifted to higher frequency than in the free benzene molecule, just as seen here, while the ν_{18} and ν_{19} bands are shifted to the red, again as seen here. The trends that we see for vibrational shifts upon metal ion binding to benzene are therefore the same as those reported before; these patterns and their origin have been discussed extensively [10,12,18]. When a transition metal binds to benzene, there is σ-donation of electron density from the molecular π cloud to empty orbitals on the metal, and also π back-bonding from the populated metal orbitals into the antibonding molecular orbitals. These effects, which are analogous to those seen for metal carbonyls and metal–olefin complexes, constitute the well-known Dewar–Chatt–Duncanson model of π-bonding [114,115]. The net result of these charge transfer processes is that the molecular bonding in the benzene is weakened, which drives many of its vibrational frequencies to lower values. This explains the red shifts seen for the ν_{18} and ν_{19} vibrational bands. The exception to this trend occurs for the ν_{11} bands, which shift to *higher* frequencies. While the red-shift is a charge transfer effect, the blue shift of ν_{11} is a mechanical effect. The presence of the metal atom over the benzene ring impedes the out-of-plane hydrogen bend. The extra repulsion at the outer turning point of this vibration produces a steeper potential in this region, which drives the frequency higher. These trends have been seen previously for condensed phase neutral di-benzene complexes [10,12,18]. Our work provides the first view of these effects for mono-benzene complexes, and allows the cations of di-benzene complexes to be compared for a wide variety of transition metals.

Another aspect of the IR spectroscopy on these complexes is that vibrations forbidden for benzene itself may become IR-active in the reduced symmetry of the metal system. For example, the ν_1 (a_{1g}) vibration (symmetric ring stretch; 992 cm^{-1}) is only Raman active in isolated benzene, but this mode is IR-active in many di-benzene complexes [10,12,18]. The assignment of vibrational structure near 1000 cm^{-1} may involve this vibrational mode in addition to the expected ν_{18} mode.

To investigate these IR spectra in more detail and to elucidate the trends in vibrational band shifts, we performed new density functional theory (DFT) calculations on these complexes [103]. Although there were many previous theoretical studies of these systems, previous work did not examine the full set of complexes for the first-row metals at the same level of theory while also focusing on the infrared spectra. Our B3LYP/6-311++G(d,p) calculations found stable minima for all the monomer and dimer metal benzene cation complexes. The schematic structures found are shown in Fig. 17; additional details about these calculations

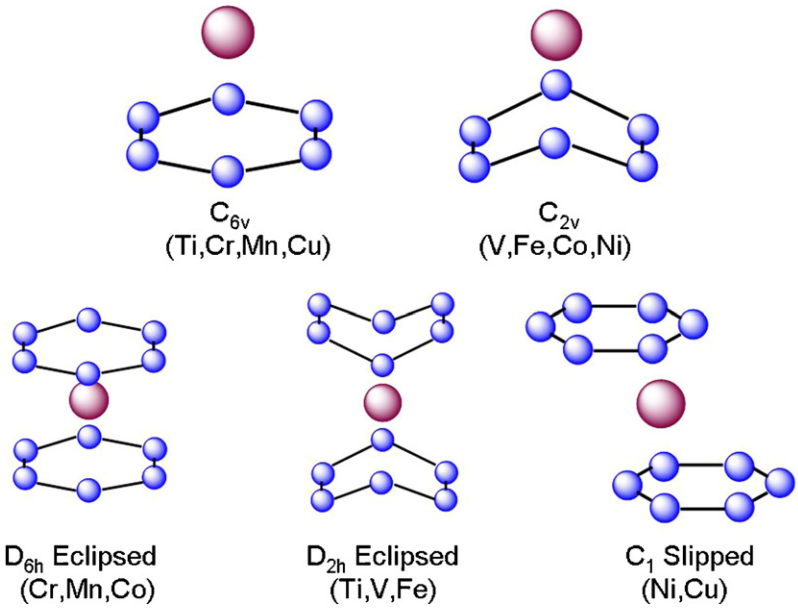

Fig. 17. The structures predicted by density functional theory computations for different metal mono- and di-benzene cation complexes.

are given in our original paper [103]. For the monomer complexes, the structures are either the simple C_{6v}, or the C_{2v} in which the benzene ring has two carbon atoms distorted slightly towards the metal. Ti^+, Cr^+, Mn^+ and Cu^+ complexes adopt the C_{6v} structure, while V^+, Mn^+, Fe^+, Co^+ and Ni^+ adopt the C_{2v} structure. Only Mn^+ exhibits both structures in different spin states. There is a noticeable trend for the more strongly bound complexes to form the C_{2v} structure. The dimer complexes may also have undistorted D_{6h} and D_{6d} structures, depending on whether the benzene rings are eclipsed or staggered with respect to each other. For several complexes, there is a negligible energy difference between the staggered and eclipsed forms. However, as in the monomers, many of the more strongly bound dimer complexes have structures in which the benzene rings are distorted. For example, a D_{2h} structure occurs for several complexes that has two carbons in each benzene ring displaced toward the metal, analogous to the monomer C_{2v} structure. A C_1 complex has the metal localized over an η^3 site on each benzene ring.

The ground electronic states in these complexes generally correspond to configurations in which the degenerate (in C_{6v}, D_{6h} and D_{6d} symmetry) $3de_2$ orbitals are occupied first, followed by the $3da_1$ orbital, and finally the $3de_1$ orbitals, which are also degenerate in C_{6v}, D_{6h} and D_{6d} symmetries. Only the quartet Fe^+-benzene monomer and dimer complexes break this rule by doubly occupying the $3da_1$ orbital before adding the fourth electron to the $3de_2$ orbitals. The dimer complexes tend to have a low spin ground state, while the monomer complexes tend to be high spin. In particular, $Ti^+(benzene)_2$ is calculated to be a doublet whereas $Ti^+(benzene)$ is a quartet; $V^+(benzene)_2$ has a triplet binding energy that is 23 kcal/mol greater than the quintet whereas the monomer triplet and quintet are within 1 kcal/mol of each other; $Cr^+(benzene)_2$ is a doublet whereas $Cr^+(benzene)$ is a sextet; $Mn^+(benzene)_2$ is a singlet whereas $Mn^+(benzene)$ is a septet; and $Fe^+(benzene)_2$ is a doublet whereas $Fe^+(benzene)$ is a quartet. The spin state for a given complex is the result of a balance between the promotion energy required to pair up the spins in the metal and the improved metal–ligand binding for paired spins. The enhanced binding for the two ligands of the dimer complexes more than compensates for the promotion energy, while the single ligand binding generally does not.

The B3LYP/6-311++G(d,p) predictions for the vibrational properties of these complexes are reported in Table 3. The bands measured in our spectrum near the positions of the benzene ν_{11} and ν_{19} bands are indeed found by theory to be the corresponding vibrations in all of the respective mono- and di-benzene complexes. Theory confirms the trends that the ν_{11} bands for the metal complexes shift to higher frequencies and that the ν_{19} bands shift to lower frequencies compared to the vibrations of free benzene. However, the quantitative agreement between theory and experiment is less satisfying. Although for some bands the agreement is close (10–20 cm^{-1}), for others the differences are as great as 50–60 cm^{-1}. The IR-REMPD bands can easily be red-shifted by 10 cm^{-1} or so from the absorption bands; consideration of this would reduce some of these discrepancies but would make others worse. Throughout these metal complexes, the ν_{11} vibrational band is predicted to have the highest IR oscillator strength of all the bands, similar to its high intensity in the IR spectrum of benzene. However, these predicted intensity differences are not apparent in the measured IR-REMPD spectra, where the ν_{11}/ν_{19} bands are often about the same size or within a factor of two. Only for the $Co^+(benzene)_{1,2}$ complexes is there a measured intensity ratio for these bands that approaches the calculated values. The intensities measured in IR-REMPD spectra depend on both the IR absorption strength and the dissociation yield. Apparently, the relative intensities of the ν_{11} bands in IR-REMPD are depressed compared to the calculated absorption intensities. However, a lower dissociation yield here is understandable because the photon energy at the ν_{11} band is lower than at the ν_{19} band, which would make dissociation require more photons on average.

Table 3
The positions of the IR bands observed for transition metal ion–benzene complexes and their comparison to the spectra of neutral complexes and to the predictions of theory

Complex	ν_{11} out-of-plane H bend		ν_1 C ring stretch (IR inactive in benzene)		ν_{18} in-plane C—H bend		ν_{19} in-plane C ring distortion	
	Exp.	Theory[a]	Exp.	Theory	Exp.	Theory[a]	Exp.	Theory[a]
C_6H_6	673	687(122)	992	979/981(0)	1038	1059/1059(6/6)	1486	1510/1510(7/7)
$Ti^+(bz)$		756(100)		899(4)		1003/1004(8/8)		1450/1450(11/11)
$Ti^+(bz)_2$	739	751(88)	946	922/974(10/19)	992	1011/1034(15/6)	1421	1466/1478/1530 (17/15/22)
$Ti(bz)_2$			946[b]		979[b]			
$V^+(bz)$	769	744[c]			980	1000/1016[c]	1425	1447/1458[c]
		791(103)		986/1001(5/11)		1005(2)		1423/1455/1528 (7/2/7)
$V^+(bz)_2$	769	724[c]	962		1005	1010/1023[c]	1449	1456/1465[c]
		761(75)		947/993(21/13)		998/1020(11/3)		1462/1535(16/58)
$V(bz)_2$	739[b]		959[b]		985[b]		1416[b]	
$Cr(bz)_2$	794[b]		971[b]		999[b]		1426[b]	
$Fe^+(bz)$		767(101)		926/931(2/2)		1004/1021(5/3)		1458/1465(16/20)
$Fe^+(bz)_2$	768	777(99)	996	955(7)		1005/1031(4/7)	1440	1453/1472(31/26)
$Co^+(bz)$	740	786(105)		929/931(1/1)		1012/1012(5/5)	1430	1456/1457(15/15)
$Co^+(bz)_2$	748	737(160)		927(2)		1023/1023(5/5)	1472	1469/1469(28/27)
$Ni^+(bz)$	744	764(105)				1005/1021(4/3)	1444	1454/1464(19/18)
$Ni^+(bz)_2$	732	733(205)		1006(1)		1021/1032(5/5)	1469	1469/1477(36/36)

All numbers are in cm^{-1}.
[a] Ref. [103], except as noted.
[b] Literature values from the condensed phase, Refs. [10,12,18].
[c] Ref. [102].

Theory can also help in the assignment of bands in the 1000 cm^{-1} region, where the IR-active ν_{18} band and the IR-forbidden ν_1 band in free benzene occur. Doublet peaks are observed here for the $Ti^+(benzene)_2$ and $V^+(benzene)_2$ complexes, and a weak feature is also seen in the $Fe^+(benzene)_2$ spectrum. As seen in Table 3, the lower frequency mode in the 1000 cm^{-1} region for the monomer and dimer complexes of Ti^+, V^+ and Fe^+ is indeed predicted to be the ν_1 mode that is IR-forbidden for benzene. This mode is calculated to have a comparable or even greater intensity than the ν_{18} band that is IR-active in benzene.

Theory can also elucidate patterns in the vibrational band shifts seen here. ν_{19} has been identified in the previous theoretical work of Chaquin and coworkers as a key indicator for the degree of metal–benzene charge transfer [37]. In the spectra shown here, both experiment and theory find substantial red shifts in the ν_{19} bands for all of these complexes. There is a general trend for the early transition metal complexes to have a greater ν_{19} red shift than the later ones. This is reasonable because the early transition metals have fewer d electrons available for π back-bonding, and so σ donation of charge toward the metal should be the dominant bonding interaction.

Another trend noted in these spectra is the *intensity* of the ν_1 vibrational bands. This band is prominent in the spectra of $Ti^+(benzene)_2$ and $V^+(benzene)_2$ complexes, but is hardly detected in any other system except $Fe^+(benzene)_2$. The ν_1 band intensity is not correlated directly with bond strength, but it appears to be correlated with the extent of charge transfer. In every case, a higher intensity for the ν_1 band parallels a strong ν_{19} red shift. Both effects are greatest in the early transition metals. It is these same complexes that also have distorted benzene, i.e., C_{2v} structures for the monomers and D_{2h} structures for the dimers. Indeed, it is this distortion that induces the IR activity in this mode. The presence of a ν_1 vibration is therefore a diagnostic for distorted benzene.

The metal spin state is a significant issue in the electronic structure of these benzene complexes, and vibrational spectra can also be used to reveal spin states. $Ti^+(benzene)_2$ provides an interesting test for this, because the $^4A_1$ and $^2B_{3g}$ configurations lie energetically within about 6 kcal/mol of each other. However, the IR spectrum was found to agree better with the pattern predicted for the quartet spin configuration, even though theory finds that the doublet is more stable [103]. A similar discrepancy was found for $V^+(benzene)_2$ [102,103]. In this case, DFT theory indicates that the triplet state is more stable than the quintet by about 25 kcal/mol. However, the vibrational spectrum matches the quintet significantly better than it does the triplet. The same effect was found by our group for $V^+(benzene)_2$ in the C—H stretching region (see below), where the quintet pattern predicted by theory also provides the best match to the spectrum [109]. This is apparently a problem with density functional theory for these systems. It is well-known that DFT has problems handling open-shell species, and it also has an intrinsic bias toward low-spin metal configurations [116].

We have also applied infrared measurements to metal ion–benzene complexes in the C—H stretching region, using our KTP/KTA OPO laser systems and the method of rare gas tagging [109,110]. Spectra for various complexes of V^+ and Ni^+ are shown in Figs. 13–16. These spectra are measured in a single photon mode of absorption, and therefore they are not subject to

the same form of power broadening and/or red-shifting that is expected to influence the IR-REMPD measurements. The clusters are produced directly as ions and then jet-cooled before the excitation. These ions are therefore expected to be colder than those produced by UV photoionization. However, the potential disadvantage of these experiments is the presence of the tag atom (argon) which may shift the spectral band positions. We therefore employ careful theoretical studies to investigate the role of the argon binding. As in the case of the studies in the fingerprint region, we are able to compare our spectra for metal ion–benzene complexes in the C–H stretching region to the well-known spectrum of benzene itself.

Fig. 13 shows the IR spectra measured for the V^+(benzene) and V^+(benzene)$_2$ complexes measured with argon tagging compared to the spectrum of V^+(benzene)$_3$ measured in the loss of benzene mass channel. The fact that benzene elimination cannot be detected from the $n=1$ or 2 complexes, but this becomes efficient at $n=3$, indicates that the $n=2$ complex has completed the coordination of the metal ion and that the extra benzene in the $n=3$ complex is external, acting essentially as a solvent molecule. Consistent with this, the spectrum also changes noticeably on going from the $n=2$ to the $n=3$ complex. The spectra for the $n=1$ and $n=2$ complexes contain a single peak in the C–H stretching region, but this becomes a more complex multiplet for the $n=3$ species. The single peak for both $n=1$ and 2 occurs at 3088 cm^{-1} with a linewidth (FWHM) of ~12 cm^{-1}. A single peak in the C–H stretching region is understandable. If the benzene moiety has a high symmetry arrangement, then essentially only one asymmetric C–H stretching motion is IR active. However, the spectra here are quite different from the pattern seen for benzene itself [113,117]. It is well-known that benzene also has only one IR-active C–H stretch (ν_{12}), but the spectrum here is perturbed by a Fermi resonance with two combination bands ($\nu_{13}+\nu_{16}$ and $\nu_2+\nu_{16}+\nu_{18}$) which fall at the same frequency, splitting the observed spectrum into a triplet. Apparently, binding to the metal ion in these complexes shifts the vibrations so that the Fermi resonance is no longer present and only the one IR-active vibration is seen. Consistent with this, theory predicts large enough differential shifts in the different vibrations to explain the loss of the Fermi resonance in the $n=1$ and 2 complexes.

The multiplet pattern seen for the $n=3$ complex is quite interesting. As shown in the figure, the band seen at 3088 cm^{-1} for the $n=1$ and $n=2$ complexes is still present here. However, in addition to this there are three new bands. Surprisingly, these bands occur at almost exactly the same positions and with the same relative intensities as the Fermi triad seen for isolated benzene. The spectrum is then a composite of that for the $n=2$ complex and one additional "free" benzene. The outer benzene that is easily eliminated by IR excitation is apparently not perturbed significantly by the presence of the metal ion, and this "solvent" molecule provides the spectral pattern of free benzene. This pattern is therefore diagnostic for the presence of un-coordinated benzene molecules in the cluster.

Fig. 14 shows an expanded view of the spectra for V^+(benzene) and V^+(benzene)$_2$ compared to the predictions of theory for these complexes. As described above, both of these vanadium ion complexes have two possible spin states that could conceivably be the ground electronic state. The low-spin triplet state is predicted by DFT to be the ground state for both of these. However, the vibrational patterns in the fingerprint region suggested that the ground state might be instead the high-spin quintet. In Fig. 14, it is shown that the triplet and quintet have different patterns expected in the C–H stretching region. Both complexes in both spin states have more than one IR-active vibration predicted because the benzene ring is distorted slightly from planarity, and this symmetry breaking turns on activity in additional bands. However, in both cases, the broad single peaks measured match those expected for the quintet species, whose tight doublets are apparently not resolved, better than those for the triplet species, whose more widely spaced multiplet could be resolved if they were present. These data again support our conclusions from the data in the fingerprint region that the ground states here are in fact quintets rather than the triplets predicted by DFT.

Fig. 15 shows the spectrum measured for Ni^+(benzene) with argon tagging. As in the case of the vanadium complexes, the mono-benzene species here is expected to have a distorted benzene ring, but the degree of distortion toward the C_{2v} structure is greater. This results in two main IR-active C–H stretches which are more shifted away from the free-benzene spectrum and more widely spaced from each other. As shown, theory and experiment are in good agreement on this predicted pattern, confirming that Ni^+(benzene) does indeed have this kind of distortion.

Fig. 16 shows the spectrum measured for Ni^+(benzene)$_2$ with argon tagging compared to the spectra predicted by theory for two different possible structures of this ion. The dashed line indicates the position calculated for the ν_{12} vibration in free benzene in the absence of the Fermi resonance. As shown, the experimental spectrum has a broad band shifted to the blue from the free-benzene band position, and this has a shoulder on the left side, perhaps indicating the presence of another unresolved band. DFT predicts a C_1 structure to have the lowest energy, but its spectrum should be a multiplet of four bands centered at about the free-benzene band position. However, a second structure identified by theory has the D_{2h} structure, with both benzene ligands buckled toward the metal ion, in the same way that ring distortion was seen for the mono-benzene complex. This structure has a predicted spectrum with two main bands that are blue shifted, and whose pattern and position match the experiment if we assume that these are not completely resolved. It would of course be desirable to have better sensitivity and resolution here, but it is apparent that the experiment agrees best with the spectrum predicted for the D_{2h} structure. In this case, DFT has apparently missed the correct qualitative structure for the complex.

Overall, it is clear that IR spectroscopy, both in the fingerprint region and in the C–H stretching region, provides enough detailed spectroscopic structure to identify specific structures of metal ion–benzene complexes, particularly with regard to ring distortion or loss of symmetry. Ring distortion is clearly evident in several of the complexes studied previously, and with the help of theory the specific structures can be identified. Ring distortion appears to be greater for the later transition metals, where

the bonding is stronger, and then the spectrum contains new IR-active bands and/or more complex multiplets. Band shifts relative to the free-benzene vibrations help to identify not only structures but specific electronic spin states in these complexes. Density functional theory has been demonstrated to be quite useful for these systems, with the caveat that it sometimes misses the correct relative energies of spin states and in some cases even the structures for these complexes. However, by comparing the specific vibrational patterns for other spin states or structures, it is usually possible to find a good interpretation of the measured spectra.

7. Future directions

As shown here, the chemistry and thermochemistry of transition metal ion–benzene complexes are well-developed areas. New directions for research on these systems will undoubtedly be in the continued application of new spectroscopy methods to these systems because of the detailed probes of electronic structure, bonding and geometries provided when vibrational structure can be measured. In this area, additional measurements of ZEKE electronic spectroscopy would be useful, as this method has only been applied to a few systems so far. An interesting question is whether the cation electronic states produced by photoionization of neutrals will always be the same as that produced when complexes are grown directly as ions. There is some indication for differences like this in the vanadium–benzene system [95], and other cases might be found.

In the infrared, better quality spectra are needed, particularly in the fingerprint region. The FEL lasers provide good output here, but the multiple photon dissociation experiments done so far have resolution too low to address many structural questions. The FEL lasers could be coupled with new ion sources allowing the rare gas tagging method to be applied here. The same spectral region could be probed with existing ion sources like those in our lab which allow efficient rare gas tagging, using the new OPO systems that go down to lower frequencies. The output pulse energies are much lower than those available with FEL's, but the sensitivity should be enough to allow such measurements. These experiments are planned in our lab. We also plan to continue tagging experiments in the C–H stretching region like those described here for vanadium and nickel systems.

It will also be interesting to apply the methods described here for substituted benzenes, where different metal ion binding sites are possible, or for more complex sandwich species containing benzene. Meijer and coworkers have investigated the attachment sites of Cr^+ ions to aniline, where ring versus nitrogen binding sites were competitive [118]. Our lab has produced a variety of mixed sandwich complexes containing benzene and other aromatic ligands such as coronene or C_{60} [74], but no spectroscopic measurements of any kind have been applied to these fascinating systems. Likewise, the multiple-decker sandwich systems produced by Kaya and Nakajima will continue to be of interest. IR spectra have been obtained for the smaller species when deposited as ions and then neutralized [65], but not for any of the multi-decker cation species in the gas phase. Of course as larger, more complex sandwich systems are studied, computational methods will have to continue to advance to complement and guide these new studies.

Acknowledgments

We gratefully acknowledge support for this work from the U.S. Department of Energy (grant no. DE-FG02-96ER14658) and the Air Force Office of Scientific Research (grant no. FA9550-06-1-0028).

References

[1] S. Winstein, H.J. Lucas, J. Am. Chem. Soc. 60 (1938) 836.
[2] R.S. Mulliken, J. Am. Chem. Soc. 74 (1952) 811.
[3] L.J. Andrews, Chem. Rev. 54 (1954) 713.
[4] H.G. Smith, R.E. Rundle, J. Am. Chem. Soc. 80 (1958) 5075.
[5] J.G. Traynham, J.R. Olechowski, J. Am. Chem. Soc. 81 (1959) 571.
[6] R. Gut, J. Rueede, J. Organomet. Chem. 128 (1977) 89.
[7] T.J. Kealy, P.L. Paulson, Nature 168 (1951) 1039.
[8] S.A. Miller, J.A. Tebboth, J.F. Tremaine, J. Chem. Soc. (1952) 632.
[9] E.O. Fischer, W.Z. Hafner, Z. Naturforsch. B 10 (1955) 665.
[10] H.R. Fritz, Adv. Organomet. Chem. 1 (1964) 239.
[11] R. Prins, F.J. Reinders, Chem. Phys. Lett. 3 (1969) 45.
[12] V.T. Aleksanyan, Vib. Spectra Struct. 11 (1982) 107.
[13] D.E. Cabelli, A.H. Cowley, J.J. Lagowski, Inorg. Chim. Acta 57 (1982) 195.
[14] E.L. Muetterties, J.R. Bleeke, E.J. Wucherer, T.A. Albright, Chem. Rev. 82 (1982) 499.
[15] M.P. Andrews, S.M. Mattar, G.A. Ozin, J. Phys. Chem. 90 (1986) 744.
[16] J.W. Caldwell, P.A. Kollman, J. Am. Chem. Soc. 117 (1995) 4177.
[17] J.C. Ma, D.A. Dougherty, Chem. Rev. 97 (1997) 1303.
[18] K. Nakamoto, Infrared, Raman Spectra of Inorganic and Organometallic Compounds, Part B, 5th ed., Wiley Interscience, New York, 1997.
[19] N.J. Long, Metallocenes, Blackwell Sciences, Ltd., Oxford, UK, 1998.
[20] P.L. Timms, R.B. King, J. Chem. Soc. Chem. Commun. (1978) 898.
[21] D.H. Russell (Ed.), Gas Phase Inorganic Chemistry, Plenum, New York, 1989.
[22] K. Eller, H. Schwarz, Chem. Rev. 91 (1991) 1121.
[23] B.S. Freiser (Ed.), Organometallic Ion Chemistry, Kluwer, Dordrecht, 1996.
[24] J.J. Leary, P.B. Armentrout (Eds.), Gas Phase Metal Ion Chemistry (Special Issue), Int. J. Mass Spectrom. 204 (2001) 1.
[25] (a) R. Wesendrup, H. Schwarz, Organometallics 16 (1997) 461; (b) K. Schroeder, C.A. Schalley, R. Wesendrup, D. Schroeder, H. Schwarz, Organometallics 16 (1997) 986.
[26] T.G. Dietz, M.A. Duncan, D.E. Powers, R.E. Smalley, J. Chem. Phys. 74 (1981) 6511.
[27] C.W. Bauschlicher, H. Partridge, S.R. Langhoff, J. Phys. Chem. 96 (1992) 3273.
[28] R.H. Hertwig, J. Hrušák, D. Schroeder, W. Koch, H. Schwarz, Chem. Phys. Lett. 236 (1995) 194.
[29] A. Ouhlal, A. Selmani, A. Yelon, Chem. Phys. Lett. 243 (1995) 269.
[30] D.J. Stöckigt, J. Phys. Chem. A 101 (1997) 3800.
[31] (a) C. Yang, S.J. Klippenstein, J. Phys. Chem. A 103 (1999) 1094; (b) S.J. Klippenstein, C. Yang, Int. J. Mass Spectrom. 201 (2000) 253.
[32] T.K. Dargel, R.H. Hertwig, W. Koch, Mol. Phys. 96 (1999) 583.
[33] R. Pandey, B.K. Rao, P. Jena, J.M. Newsam, Chem. Phys. Lett. 321 (2000) 142.
[34] G. Hong, M. Dolg, L. Li, Int. J. Quant. Chem. 80 (2000) 201.
[35] M. Dolg, J. Chem. Inf. Comput. Sci. 41 (2001) 18.
[36] R. Pandey, B.K. Rao, P. Jena, M.A. Blanco, J. Am. Chem. Soc. 123 (2001) 3799.
[37] P. Chaquin, D. Costa, C. Lepetit, M. Che, J. Phys. Chem. A 105 (2001) 4541.

[38] M. Kaczorowska, J.M. Harvey, Phys. Chem. Chem. Phys. 4 (2002) 5227.
[39] J. Molina, J.A. Dobado, S. Melchor, Theochem 589 (2002) 337.
[40] M. Diefenbach, C. Trage, H. Schwarz, Helv. Chim. Acta 86 (2003) 1008.
[41] D. Kim, S. Hu, P. Tarakeshwar, K.S. Kim, J.M. Lisy, J. Phys. Chem. A. 107 (2003) 1228.
[42] Y. Mokrousov, N. Atodiresei, G. Bihlmayer, S. Bluegel, Int. J. Quant. Chem. 106 (2006) 106.
[43] T.D. Jaeger, M.A. Duncan, Int. J. Mass Spectrom. 241 (2005) 165.
[44] P. Fayet, L. Woeste, Surf. Sci. 156 (1985) 134.
[45] P. Schnabel, M.P. Irion, K.G. Weil, J. Phys. Chem. 95 (1991) 9688.
[46] (a) R.J. St. Pierre, M.A. El-Sayed, J. Phys. Chem. 91 (1987) 763;
(b) R.J. St. Pierre, E.L. Chronister, M.A. El-Sayed, J. Phys. Chem. 91 (1987) 5228.
[47] (a) M.R. Zakin, D.M. Cox, A. Kaldor, J. Phys. Chem. 91 (1987) 5224;
(b) M.R. Zakin, R.O. Brickman, D.M. Cox, A. Kaldor, J. Chem. Phys. 88 (1988) 5943.
[48] H. Higashide, T. Kaya, M. Kobayashi, H. Shinohara, H. Sato, Chem. Phys. Lett. 171 (1990) 297.
[49] C. Berg, M. Beyer, U. Achatz, S. Joos, G. Niedner-Schatteburg, V.E. Bondybey, J. Chem. Phys. 108 (1998) 5398.
[50] K. Hoshino, T. Kurikawa, H. Takeda, A. Nakajima, K. Kaya, J. Phys. Chem. 99 (1995) 3053.
[51] K. Hoshino, T. Kurikawa, H. Takeda, A. Nakajima, K. Kaya, Surf. Rev. Lett. 3 (1996) 183.
[52] T. Yasuike, A. Nakajima, S. Yabushito, K. Kaya, J. Phys. Chem. A 101 (1997) 5360.
[53] A. Nakajima, K. Kaya, J. Phys. Chem. A 104 (2000) 176.
[54] K. Kaya, S. Nagao, Y. Negishi, K. Judai, A. Kato, Y. Nakamura, A. Nakajima, Clusters Nanostruct. Interf. (2000) 301.
[55] T. Kurikawa, H. Takeda, M. Hirano, K. Judai, T. Arita, S. Nagoa, A. Nakajima, K. Kaya, Organometallics 18 (1999) 1430.
[56] A.K. Kandalam, B.K. Rao, P. Jena, J. Chem. Phys. 120 (2004) 10414.
[57] J. Wang, P.H. Acioli, J. Jellinek, J. Am. Chem. Soc. 127 (2005) 2812.
[58] J. Wang, J. Jellinek, J. Phys. Chem. A 109 (2005) 10180.
[59] J. Kua, K.M. Tomlin, J. Phys. Chem. A 110 (2006) 11988.
[60] P. Weis, P.R. Kemper, M.T. Bowers, J. Phys. Chem. A 101 (1997) 8207.
[61] K. Miyajima, A. Nakajima, S. Yabushita, M.B. Knickelbein, K. Kaya, J. Am. Chem. Soc. 126 (2004) 13202.
[62] K. Miyajima, S. Yabushita, M.B. Knickelbein, A. Nakajima, J. Am. Chem. Soc. 129 (2007) 8473.
[63] K. Miyajima, M.B. Knickelbein, A. Nakajima, Eur. Phys. J. D 34 (2005) 177.
[64] K. Judai, K. Sera, S. Amatsutsumi, K. Yagi, T. Yasuike, S. Yabushita, A. Nakajima, K. Kaya, Chem. Phys. Lett. 334 (2001) 277.
[65] (a) S. Nagaoka, E. Okada, S. Doi, M. Mitsui, A. Nakajima, Eur. Phys. J. D 34 (2005) 239;
(b) S. Nagaoka, T. Matsumoto, K. Ikemoto, M. Mitsui, A. Nakajima, J. Am. Chem. Soc. 129 (2007) 1528.
[66] R.L. Hettich, T.C. Jackson, E.M. Stanko, B.S. Freiser, J. Am. Chem. Soc. 108 (1986) 5086.
[67] R.L. Hettich, B.S. Freiser, J. Am. Chem. Soc. 109 (1987) 3537.
[68] J.R. Gord, B.S. Freiser, S.W. Buckner, J. Chem. Phys. 94 (1991) 4282.
[69] S. Afzaal, B.S. Freiser, Chem. Phys. Lett. 218 (1994) 254.
[70] E.D. Pillai, K.S. Molek, M.A. Duncan, Chem. Phys. Lett. 405 (2005) 247.
[71] K.F. Willey, P.Y. Cheng, K.D. Pearce, M.A. Duncan, J. Phys. Chem. A 94 (1990) 4769.
[72] K.F. Willey, P.Y. Cheng, M.B. Bishop, M.A. Duncan, J. Am. Chem. Soc. 113 (1991) 4722.
[73] K.F. Willey, C.S. Yeh, D.L. Robbins, M.A. Duncan, J. Phys. Chem. 96 (1992) 9106.
[74] J.W. Buchanan, G.A. Grieves, J.E. Reddic, M.A. Duncan, Int. J. Mass Spectrom. 182 (1999) 323.
[75] S.G. Lias, in: P.J. Linstrom, W.G. Mallard (Eds.), NIST Chemistry WebBook, NIST Standard Reference Database Number 69, National Institute of Standards and Technology, Gaithersburg, MD, 20899, 2007.
[76] B.J. Whitaker (Ed.), Imaging in Molecular Dynamics, Cambridge University Press, UK, 2003.
[77] M.N.R. Ashfold, N.H. Nahler, A.J. Orr-Ewing, O.P.J. Vieuxmaire, R.L. Toomes, T.N. Kitsopoulos, I.A. Garcia, D.A. Chestakov, S.M. Wu, D.H. Parker, Phys. Chem. Chem. Phys. 8 (2006) 26.
[78] Y.M. Chen, P.B. Armentrout, Chem. Phys. Lett. 210 (1993) 123.
[79] P.B. Armentrout, D.A. Hales, L. Lian, in: M.A. Duncan (Ed.), Adv. Metal & Semicon. Clusters, vol. 2, JAI Press, Greenwich, CT, 1994, p. 1.
[80] F. Meyer, F.A. Khan, P.B. Armentrout, J. Am. Chem. Soc. 117 (1995) 9740.
[81] M.T. Rogers, P.B. Armentrout, Mass Spectrom. Rev. 19 (2000) 215.
[82] R.C. Dunbar, in: L.M. Babcock an, N.G. Adams (Eds.), Advances in Gas Phase Ion Chemistry, vol. 2, JAI Press, Greenwich, CT, 1996, p. 87.
[83] C.-Y. Lin, R.C. Dunbar, Organometallics 16 (1997) 2691.
[84] Y.-P. Ho, Y.-C. Yang, S.J. Klippenstein, R.C. Dunbar, J. Phys. Chem. A 101 (1997) 3338.
[85] Y.-P. Ho, R.C. Dunbar, Int. J. Mass Spectrom. 182/183 (1999) 175.
[86] D. Schroeder, J. Hrušák, R.H. Hertwig, W. Koch, P. Schwerdtfeger, H. Schwarz, Organometallics 14 (1995) 312.
[87] Y. Li, T. Baer, J. Phys. Chem. A 106 (2002) 9820.
[88] K. Judai, M. Hirano, H. Kawamata, S. Yabushita, A. Nakajima, K. Kaya, Chem. Phys. Lett. 270 (1997) 23.
[89] M. Gerhards, O.C. Thomas, J.M. Nilles, W.-J. Zheng, K.H. Bowen Jr., J. Chem. Phys. 116 (2002) 10247.
[90] W. Zheng, J.M. Nilles, O.C. Thomas, K.H. Bowen Jr., J. Chem. Phys. 122 (2005) 044306.
[91] W. Zheng, J.M. Nilles, O.C. Thomas, K.H. Bowen Jr., Chem. Phys. Lett. 401 (2005) 266.
[92] E.W. Schlag, ZEKE Spectroscopy, Cambridge University Press, 1998.
[93] B.R. Sohnlein, S. Li, D.-S. Yang, J. Chem. Phys. 123 (2005) 214306.
[94] B.R. Sohnlein, D.-S. Yang, J. Chem. Phys. 124 (2006) 134305.
[95] B.R. Sohnlein, Y. Lei, D.-S. Yang, J. Chem. Phys. 127 (2007) 114302.
[96] V.N. Bagratashvili, V.S. Letekov, A.A. Makarov, E.A. Ryabov, Multiple Photon Infrared Laser Photophysics and Photochemistry, Harwood Academic Publishers, Chur, 1985.
[97] L.R. Thorne, J.L. Beauchamp, in: M.T. Bowers (Ed.), Gas Phase Ion Chemistry, vol. 3, Academic Press, Orlando, FL, 1984, p. 41.
[98] R.C. Dunbar, Int. J. Mass Spectrom. 200 (2000) 571.
[99] T. Baer, W.L. Hase, Unimolecular Reaction Dynamics, Oxford University Press, 1996.
[100] G. von Helden, D. van Heijnsbergen, G. Meijer, J. Phys. Chem. A 107 (2003) 1671.
[101] J. Oomens, B.G. Sartakov, G. Meijer, G. von Helden, Int. J. Mass Spectrom. 254 (2006) 1.
[102] D. van Heijnsbergen, G. von Helden, G. Meijer, P. Maitre, M.A. Duncan, J. Am. Chem. Soc. 124 (2002) 1562.
[103] T.D. Jaeger, D. van Heijnsbergen, S.J. Klippenstein, G. von Helden, G. Meijer, M.A. Duncan, J. Am. Chem. Soc. 126 (2004) 10981.
[104] (a) L.I. Yeh, M. Okumura, J.D. Myers, J.M. Price, Y.T. Lee, J. Chem. Phys. 91 (1989) 7319;
(b) M. Okumura, L.I. Yeh, J.D. Myers, Y.T. Lee, J. Phys. Chem. 94 (1990) 3416.
[105] T. Ebata, A. Fujii, N. Mikami, Int. Rev. Phys. Chem. 17 (1998) 331.
[106] E.J. Bieske, O. Dopfer, Chem. Rev. 100 (2000) 3963.
[107] W.H. Robertson, M.A. Johnson, Ann. Rev. Phys. Chem. 54 (2003) 173.
[108] M.A. Duncan, Int. Rev. Phys. Chem. 22 (2003) 407.
[109] T.D. Jaeger, E.D. Pillai, M.A. Duncan, J. Phys. Chem. A 108 (2004) 6605.
[110] T.D. Jaeger, M.A. Duncan, J. Phys. Chem. A 109 (2005) 3311.
[111] Designed and sold by Dean Guyer, LaserVision, Inc., Bellevue, WA, USA.
[112] (a) M. Gerhards, C. Unterberg, A. Gerlach, Phys. Chem. Chem. Phys. 4 (2002) 5563;
(b) M. Gerhards, Opt. Commun. 241 (2004) 493.
[113] T. Shimanouchi, in: P.J. Linstrom, W.G. Mallard (Eds.), Molecular Vibrational Frequencies, NIST Chemistry WebBook, NIST Standard Reference Database Number 69, National Institute of Standards and Technology, Gaithersburg, MD, 20899, http://webbook.nist.gov, 2007.

[114] J. Chatt, L.A. Duncanson, J. Chem. Soc. (1953) 2939.
[115] M.J.S. Dewar, S. Bull. Soc. Chim. Fr. 18 (1951) C79.
[116] W. Koch, M.C. Holthausen, A Chemist's Guide to Density Functional Theory, 2nd ed., Wiley-VCH, Weinheim, 2001.
[117] D.L. Snavely, V.A. Walters, S.D. Colson, K.B. Wiberg, Chem. Phys. Lett. 103 (1984) 423.
[118] J. Oomens, D.T. Moore, G. von Helden, G. Meijer, R.C. Dunbar, J. Am. Chem. Soc. 126 (2004) 724.